Geophysical mapping of groundwater properties for transport infrastructure construction planning - Final report

Martin, Tina; Dahlin, Torleif; Mendoza, Alfredo; Kass, Andrew

2022

Document Version:
Publisher's PDF, also known as Version of record

GEOPHYSICAL MAPPING OF GROUNDWATER PROPERTIES FOR TRANSPORT INFRASTRUCTURE CONSTRUCTION PLANNING

Tina Martin,
Torleif Dahlin,
Alfredo Mendoza,
Andrew M. Kass

REPORT 2022-12

Engineering Geology
Faculty of Engineering
Lund University

GEOPHYSICAL MAPPING OF GROUNDWATER PROPERTIES FOR TRANSPORT INFRASTRUCTURE CONSTRUCTION PLANNING

Final report for project TRV 2020/122405

LUND UNIVERSITY

LTH
FACULTY OF ENGINEERING

Lund, 2022-12-21

T. Martin, T. Dahlin, A. Mendoza, A.M. Kass
tina.martin@tg.lth.se

Summary

The success and costs of infrastructure projects largely depend on reliable characterization of the subsoil, where information on groundwater is essential to protect groundwater resources and to avoid stability problems. To determine the hydrogeological characteristics, drilling is carried out followed by hydraulic tests which are reliable but expensive and provide limited information which, in some cases, may not be representative of the entire area that may be affected. The use of geophysical methods can overcome this problem and by providing continuous information that can be used to optimize well placement and execution. The results of the drilling and hydraulic tests can then in turn be fed back to improve the interpretation of the geophysical results. It is thereby possible to get more comprehensive and relevant results that reduce the risk of problems in the construction phase, thus saving resources, time and costs.

The geoelectrical method DCIP (Direct Current resistivity and time-domain Induced Polarization) can provide information on the intrinsic permeability. In addition, MRS (Magnetic Resonance Sounding) can provide information on the water content and properties of the pore spaces, and thus also information related to the hydraulic conductivity. By combining both methods and using them in a two- or three-dimensional layout, a more comprehensive description of the subsoil is possible.

The purpose of the project is to find out how both methods can contribute to a reliable characterisation of the subsoil's hydrogeological properties. The methods were tested alongside conventional tests of the hydraulic conductivity using boreholes, slug tests and HPT (hydraulic profiling tool) to investigate three different test sites. The test sites were chosen to reflect different hydrogeological conditions and to provide access to reference data. Furthermore, their electromagnetic noise level was a crucial factor as it can affect the geophysical results. Measured data were processed, interpreted and compared, to evaluate the geophysical results with regard to hydrogeological information value, as well as robustness in measurement environments with different signal interference conditions.

The results show that DCIP tomography provided inverted depth sections with hydraulic conductivity along the survey lines that mostly agree with the reference data from conventional methods at all three test locations. They also show that DCIP is robust enough to give good results along all test lines performed. However, it is not a guarantee that the method works everywhere due to the presence of noise/disturbances, for example in urban environments. It should also be mentioned that the algorithms that have been used for the interpretation of the hydraulic properties are part of research software, and that there is great potential for further development but also a need to adapt the user interface for a wider use. The results also show that MRS can provide information on water content and hydraulic properties that are mainly consistent with the reference data from other methods, thereby providing valuable complementary information. However, MRS measured from the ground surface, as tested here,

is significantly more sensitive to electromagnetic interference, which was manifested in the fact that the method only worked fully at one of the test sites while giving limited or no useful results at the other test sites, due to the presence of noise generated by adjacent infrastructure.

Sammanfattning

Framgången och kostnaderna för infrastrukturprojekt beror till stor del på tillförlitlig karakterisering av undermarken. Speciellt är information om grundvattnet avgörande för att skydda grundvattenresurserna och för att undvika stabilitetsproblem. För att fastställa de hydrogeologiska egenskaperna genomförs borrningar följt av hydrauliska tester som är tillförlitliga men dyra, och det ger endast punktinformation som kanske inte är representativ för hela det område som kan komma att påverkas. Användningen av geofysiska metoder kan övervinna detta problem och kontinuerlig information som kan användas till att optimera borrningarnas placering och utförande. Resultaten av borrningarna och de hydrauliska testerna kan sedan i sin tur återkopplas för att förbättra tolkningen av de geofysiska resultaten. Man kan därigenom få mera heltäckande och relevanta resultat som minskar risken för problem i byggskedet, och därmed spara resurser, tid och kostnader.

Den geoelektriska metoden DCIP (Direct Current resistivity and time-domain Induced Polarisation) kan ge information om den hydrauliska konduktiviteten. Dessutom kan MRS (Magnetic Resonance Sounding) ge information om vatteninnehåll och egenskaper för porutrymmena, och därmed även information relaterad till den hydrauliska konduktiviteten. Genom att kombinera båda metoderna och använda dem i ett två- eller tredimensionellt upplägg är en mer heltäckande beskrivning av undermarken möjlig.

Syftet med projektet är att ta reda på hur båda metoderna kan bidra till en tillförlitlig karakterisering av undermarkens hydrogeologiska egenskaper. Metoderna testades tillsammans med konventionella tester av den hydrauliska konduktiviteten med hjälp av borrningar och slugtester för att undersöka tre olika testplatser. Testplatserna valdes för att avspegla olika hydrogeologsiak förhållanden samt att ge tillgång till referensdata. Vidare var deras elektromagnetiska brusnivå en avgörande faktor eftersom den kan påverka de geofysiska resultaten. Uppmätta data bearbetades, tolkades och jämfördes, för att utvärdera de geofysiska resultaten med avseende på hydrogeologiskt informationsvärde, samt robusthet i mätmiljöer med olika signalstörningsförhållanden.

Resultaten visar att DCIP tomografi gav inverterade djupsektioner med hydraulisk konduktivitet längs undersökningslinjerna som stämmer överens med resultaten från slugtest och HPT (hydraulic profiling tool) på samtliga tre testlokaler. De visar också att metoden är tillräckligt robust för att ge bra resultat längs alla utförda testlinjer. Detta är dock inte en garanti för att metoden fungerar överallt, exempelvis i utpräglat urbana miljöer. Det bör också nämnas att de algoritmer som har använts för tolkningen av de hydrauliska egenskaperna ingår i forskningsprogramvaror, och att det finns stor potential för vidareutveckling men också behov av anpassning av användargränssnitt för en bredare användning. Resultaten visar också att MRS kan ge information om vatteninnehåll och hydrauliska egenskaper som är i samklang med referensdata från andra metoder, och därigenom ge värdefull kompletterande information. MRS mätt från markytan, såsom den testades här, är dock betydligt mera känslig för

elektromagnetiska störningar, vilket manifesterades i att metoden bara fungerade fullt ut på en av testlokalerna medan den gav begränsade respektive inga användbara resultat på de andra testlokalerna.

Introduction and background

Construction of transport infrastructure often involves extensive excavation work. For that it is crucial to know the groundwater conditions since, for example, (i) leaking groundwater can affect stability and require unplanned measures, (ii) the lowering of groundwater levels can negatively affect groundwater bodies, groundwater sources and ecosystems, (iii) groundwater lowering can cause subsidence in buildings and other infrastructure, (iv) increased groundwater gradients can lead to the transport of pollutants from contaminated land or (v) groundwater lowering can lead to oxidation of pollutants and naturally occurring substances that can later be transported with the groundwater.

It is also necessary to assess the need for protective measures for groundwater resources and groundwater sources in connection with and during the construction of transport infrastructure. Since protective measures can be very costly, it is important to have good knowledge of the spatial location of groundwater resources and the distribution of geomaterials with different hydrogeological properties, so that the right measures are taken.

Determination of the hydrogeological properties is needed to be able to make realistic calculations of the construction effects. Today, these are determined by means of drilling accompanied by sieve analysis, slug, or pumping tests. But these tests provide limited information, are time-consuming and are usually quite costly.

Geophysical methods as, for example, ERT (Electric Resistivity Tomography) is nowadays routinely used in preliminary investigations for infrastructure projects and for hydrogeological mapping. The method maps the spatial distribution of the resistivity in the underground, and depending on the measurement setup, ERT can provide two-dimensional (2D) or three-dimensional (3D) models of the electrical properties. By varying the electrode distance and the size of the electrode layouts, one can vary the resolution and depth of penetration for the method. Using geological reference data from the area, these features can be interpreted in geological, hydrogeological and geotechnical terms (Rønning et al. 2013; Danielsen and Dahlin 2009; Ganerød et al. 2006; Dahlin 2001).

In addition to ERT, it is possible to measure DCIP (Direct Current resistivity and time-domain Induced Polarization) tomography, which gives a measure of the soil's charging capacity in addition to the resistivity distribution. The chargeability controls the frequency dependent electrical properties, and if you determine these over a wide frequency or time range it is called Spectral Induced Polarization (SIP). SIP has traditionally been performed using frequency-based measurement in the laboratory since it provides high accuracy data, but the development in recent years have made it possible to use DCIP for SIP (Olsson et al. 2016) which means that the field measurements can be carried out in a more time- and cost-effective way. It has also been shown that DCIP can be used to determine the soil's hydraulic conductivity, and thus provide spatial information about the soil's hydrogeological properties (Maurya et al. 2018).

Another geophysical method, MRS (Magnetic Resonance Sounding), can provide a measure of the free water content (reservoir coefficient in open reservoir), as well as the pore size distribution (which links to hydraulic transmissivity) as a function of depth, without drilling and hydrogeological tests (Perttu 2011; Kirsch 2009; Lachassagne et al. 2005). MRS is traditionally time-consuming to measure, so that in practice it has only been possible to make one sounding per day (which in itself is advantageous compared to drilling accompanied by hydraulic tests). This method is also very sensitive to electromagnetic interference from, for example, power grids and buried cables, which has limited its usefulness. However, development of the measurement and signal processing technology has made it possible to speed up the measurement process while the method becomes more robust against signal disturbances (Liu et al. 2019a; Liu et al. 2019b), which opens new application possibilities.

Methods and test sites

Direct current resistivity and induced polarisation (DCIP)

Electrical resistivity tomography (ERT) is based on galvanic measurement of the underground's resistivity, or specific resistance, which is done by sending a current between two electrodes and measuring the potentials generated between two other electrodes. The resistivity mainly depends on the water and fine material content in the soil, as well as the ion content of the water. Different depths of penetration are achieved by varying the electrode spacing, and measurement with many different electrode spacings along a line or across a surface can be used to create models in 2D and 3D respectively.

Induced Polarization (IP) is based on galvanic measurement of the frequency dependence of the resistivity and is thus an extension of the resistivity method. The IP effects can be explained by electrochemical phenomena in the soil, and variations in IP properties can under certain conditions be linked to hydrogeological properties (Weller and Slater 2019). The measurements can be performed in the frequency domain or time domain, where the latter can be done with instruments for resistivity measurement (Martin et al. 2020).

If the IP measurement is made with sufficiently wide time or frequency content, it is called spectral IP. Newly developed technology allows combined ERT and IP measurement, often called DCIP (Direct Current resistivity and time-domain Induced Polarization), to provide spectral IP data. It has been demonstrated at both laboratory and field scale that it is possible to quantify hydrogeological properties from spectral DCIP data (Weller et al. 2015, Maurya et al. 2018).

Magnetic resonance sounding (MRS)

Magnetic resonance sounding (MRS) is based on strong electromagnetic fields being sent out using a cable loop (coil). The principle of the method is well-known and used as a standard tool in medicine and physics. It is based on the hydrogen protons in water molecules being set into oscillation. The frequency of the emitted electromagnetic field is adjusted according to the strength of the local earth's magnetic field, so that it corresponds to the precession frequency of the hydrogen. The strength of the fields induced by the oscillations of the hydrogen, and their decay, is measured, which can be related to the content of freely moving water in the soil. By varying the strength of the transmitted current, the depth penetration is varied. As a result, MRS can provide information on the amount of water, hydraulic conductivity, and pore space structure (Perttu 2011; Kirsch 2009; Lachassagne et al. 2005). In order to be able to interpret MRS data quantitatively, knowledge of the resistivity distribution in the soil is required, which is obtained from e.g., ERT or DCIP tomography.

For the interpretation of data from both ERT, DCIP and MRS, so-called inversion (inverse numerical model interpretation) is used. Inversion is the process of finding a model of the investigated underground with the distribution of physical properties (e.g., resistivity or water

content) through an iterative procedure so that the (calculated) model response matches the measured data as closely as possible. The finite element method (FEM) is often used for the model calculation.

HPT & slug tests

Slug tests are used for quantifying hydraulic conductivity which provide a measure of the properties in the tested borehole's immediate surroundings. Pumping tests require several separate observation boreholes and gives information related to a larger volume. In the last 10 years also the hydraulic profiling tool (HPT) has become a method for the hydraulic investigation of soils and unconsolidated formations (McCall & Christy 2020). Here, water is injected into the formation while it is steadily advanced into the subsurface. A downhole pressure sensor detects the pressure that is needed to inject the water in the formation. A up-hole flowmeter monitors the water flow rate. That enables high-resolution detection of relative vertical changes in the formation's hydraulic conductivity. Post-processing allows for the calculation of the corrected HPT pressure and the estimation of the hydraulic conductivity within certain limits (McCall & Christy 2020).

Instrumentation and measurement settings for the field measurements

For the DCIP measurements at all test sites the same cable layout and instrument settings have been used. To avoid electromagnetic noise at early decay times, separated multi electrode cables for the current transmission and voltage measurements have been deployed. We used the ABEM Terrameter LS2 instrument with an Electrode Selector ES10-64C and measured with a multiple-gradient array in the IP100% mode. The pulse length was always 4s (1.6s delay time + 2.4s acquisition time). The used spread and protocol files were *2xShortShift1.xml* and *GDsepCD82.xml*. In Figure 1 some photos of the DCIP setup can be seen.

The coordinates for each DCIP electrode were measured with differential GNSS. Due to technical difficulties, only selected electrode positions could be measured for profile 1 in Mjölkalånga.

Figure 1: DCIP field setup with the different multi electrode cables and the ABEM Terrameter LS2 instrument.

To measure MRS, the ASPU system developed at Aarhus University was primarily used with a transmit/receiver loop of 50m x 25m figure-8 shape. The orientation was determined by the local noise field. More information about the MRS measurements can be found in the attached reports from Aarhus University.

Data processing and inversion

The processing of the data was done in three steps: first, a processing tool was applied on the full waveform data for (e.g.) background and spike removal and denoising (see Olsson et al. 2016). Thereafter, an automatic tool to remove bad data was used (not yet published software by Anders Kühl/Aarhus University), followed by a hand-processing. The clean data was then inverted with the inversion tool *AarhusInv* developed by Aarhus University, Denmark.

The estimation of the intrinsic permeability from the DCIP data was done directly in the *AarhusInv* software (Maurya et al. 2018). The calculation of the intrinsic permeability is based on equations that were acquired from laboratory data on unconsolidated samples (Weller et al. 2015). They proposed that for unconsolidated sediments, a link between the intrinsic permeability *k* and the imaginary electrical conductivity σ'' exists. The latter one can be

calculated from the measured IP parameters resistivity ρ and phase ϕ respectively chargeability m. *k* can be then calculated by

$$k = \frac{3.47 \times 10^{-16}\, \sigma_0^{1.11}}{\sigma''^{2.41}} \quad \text{(eq. 1)}$$

With k in [m^2], σ_0 being the DC electrical conductivity in [mS/m] and σ'' the above mentioned imaginary electrical conductivity in [mS/m] (Fiandaca et al. 2018).

This calculated intrinsic permeability can then be converted to hydraulic conductivity *K* [m/s] values by

$$K = k \cdot \frac{\rho \cdot g}{\eta} \quad \text{(eq. 2)}$$

where *k* is the intrinsic permeability in m^2, ρ is the water density, g is the gravitational acceleration in m/s^2 and η is the water viscosity in Pa·s. Under the assumption of a water density of 1000 kg/m^3, a viscosity of 10^{-3} Pa s and g≈10 m/s^2 the conversion factor is close to 10^7. This conversion we have used to compare the intrinsic permeability calculated from DCIP and the hydraulic conductivity values won from slug tests.

In addition to the above-mentioned method, Fiandaca et al. (2021) have developed another algorithm that directly inverts the DICP results into hydraulic conductivity K. It has been shown that this has resulted in a good agreement between the hydraulic conductivities won from slug tests and from DCIP data at six different European test sites (Martin et al. 2021). Unfortunately, the software is not yet commercially available so only one profile could be inverted (for testing – not shown here).

Besides these both approaches, we started to work on another approach for the estimation of the hydraulic properties that can be used for frequency- and time domain spectral data and calculates the intrinsic permeability and hydraulic conductivity after transforming it to a Debye distribution. One first example of a good fit of hydraulic conductivity for one profile in Mjölkalånga can be seen in Figure 22. That research needs to be continued and tested on a broader range of test site.

Test sites

The measurements in the project took place at three different test sites in Sweden. These sites were chosen regarding their varying (hydro-)geology, their electromagnetic noise level, their relevance for infrastructure projects, their accessibility, and the availability of reference data. At each tests site several DCIP profiles and MRS soundings were conducted. At the first two test sites, Börringe and Hasslerör, previous reported punctual hydraulic data was available. At the third site in Mjölkalånga additional HPT and slug tests were conducted by the Danish company NIRAS.

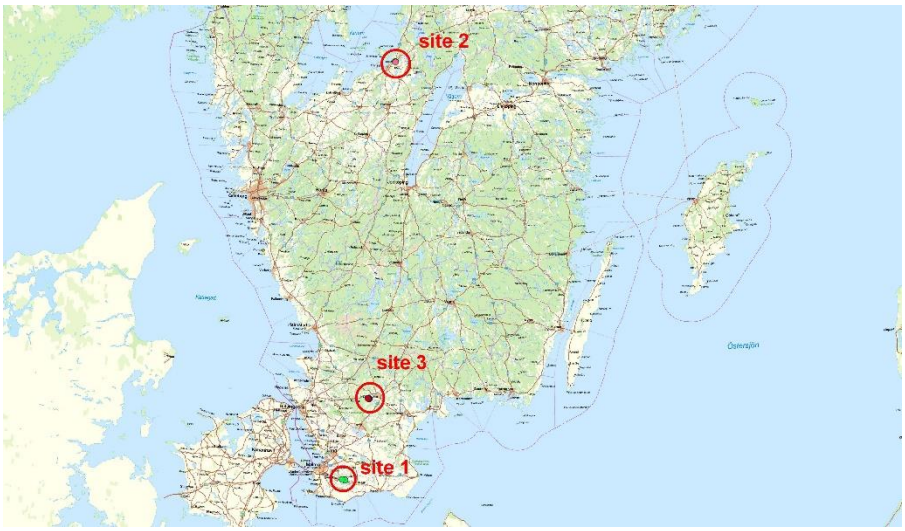

Figure 2: Map of South Sweden with an overview about the three investigated test sites. Site 1: Börringe – close to Svedala, site 2: Hasslerör – close to Mariestad, site 3: Mjölkalånga – close to Hässleholm.

Test site 1: Börringe/Svedala

Several areas in (and close to) Börringe were measured with DCIP and MRS. Here, a new track for the E65 is planned by Trafikverket and will be realised in the upcoming years. Geotechnical information, together with hydraulic data from 2017, was available via a report from Trafikverket (TRV 2020a). The different measurement areas were chosen regarding their soil types. Clay till dominates at the site, interlayered in some cases by sand till and locally covered by organic soils (peat). At area B (see Figure 3) a thick clay till layer is expected to extend up to the surface. Area C is covered by peat whereas area A is characterised by sand till and clay till. The hydraulic conductivities, won from slug tests, varied between $1.9*10^{-6}$ m/s (area A) and $2.1*10^{-9}$ m/s (area B) in 2017. The groundwater depth was between 2 and 3 m below surface in 2017 (area A). In May 2021, most of the groundwater boreholes were not visible anymore. In area B the groundwater depth was 4.9 m below surface in 2021 and at area C 0.91 m below surface (see also Table 1 and Figure 3).

Table 1: Description of test site 1: Börringe

Area	Well	Hyd. Conductivity *K* from slug test	GW depth (2017)	GW depth (Nov 2021)	Description
A	AF 67, AF 148 AF 152	$1.9*10^{-6}$ m/s $1.7*10^{-7}$ m/s $2.4*10^{-7}$ m/s	-2.6m -2m -3m	Stuck Not visible Not visible	ClTi, SaTi (up to -9m) ClTi, SaTi (up to -11m) ClTi (up to -7.5m)
B	AF 108	$2.1*10^{-9}$ m/s	?	-4.9m	ClTi (up to -8m)
C	-			-0.91m	Peat area (P, L, Med)

The geophysical soundings and profiles were chosen regarding the available boreholes and respective hydraulic conductivity information as well as for their distance from the road and power lines. We measured 10 DCIP profiles in Börringe in May 2021 at area A and B. At area A, six parallel profiles (A148P1a/b – A148P5) and one transversal profile (A148Px) were measured. For each profile, we used 82 electrodes at a separation of a = 2m. Two of the parallel profiles (A148P1a and A148P1b) were measured on the same spot but with a one-meter lateral offset, so a higher resolution profile could be obtained. The wells AF 67, AF 148, AF152 were crossed in area A and well AF 108 in area B (see also Table 2).

Table 2: DCIP profile parameter for test site 1 - Börringe.

Area	Name of profile	Profile length [m]	Electrode distance a [m]	Crosses well at …profile m
A	Profile A148 P1a-P5	162	2	AF152 at **21m**
A	Profile A148 P1x	162	2	AF148 at **78m**
A	Profile A67 P1	162	2	AF67 at **64m**
B	Profile B108 P1	162	2	AF108 at **81m**
B	Profile B108 Px	162	2	AF108 at **81m**

Several MRS soundings were conducted at site 1 in October 2021 (see green dots in Figure 3). However, the presence of the large powerline subparallel to the highway contaminated most of the measurements. In general, low free water content at most spots have resulted in too low signals. Only in the peat area C a usable line of data was obtained. More information can be found in the attached report form Aarhus University.

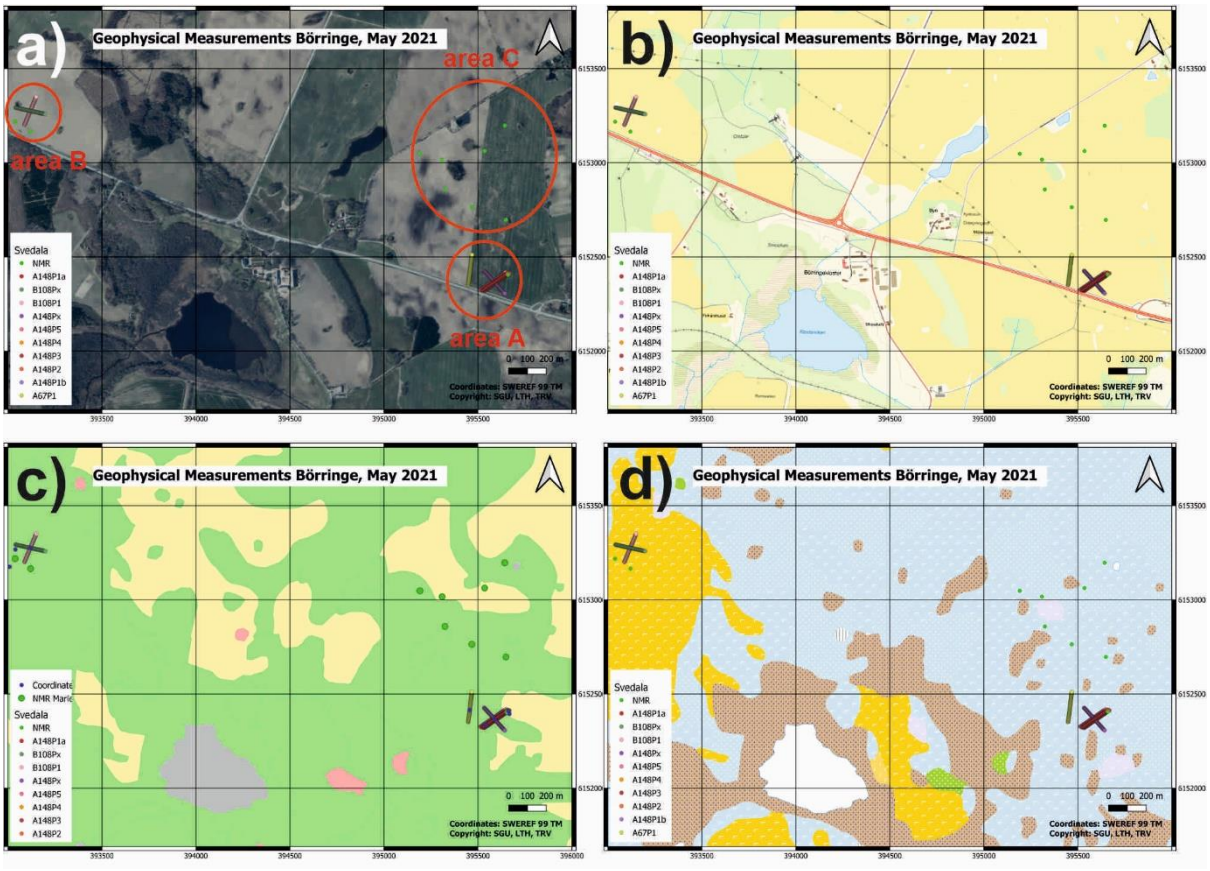

Figure 3: DCIP Profiles (coloured lines) and MRS soundings (green dots) plotted on a a) satellite map, b) topographic map, c) groundwater vulnerability map, d) soil characteristic map. In c) the groundwater reservoir is high (area A and C) respectivly medium (area B). In d) area B is characterised by postglacial fine clay, area A by clayey till. Area C is also characterised by peat spots. The scale for groundwater vulnerability and soil characteristic can be seen in Figure 4.

Figure 4: Legend for soil types and groundwater vulnerability in Figure 3, Figure 5 and Figure 6 (c and d).

Test site 2: Hasslerör/Mariestad

Test site 2 is located in Hasslerör, close to Mariestad. Here, at the Hasslerör interchange, an underpass is planned for a road under the E20 by Trafikverket. Also, a new bridge is projected across the E20. Geotechnical investigations were carried out in 2020 with hydrogeological data in some areas (TRV 2020b). The geology of the test site is characterised by sand till covered by glacial and postglacial clay and silt, and the presence of glaciofluvial deposits, which also includes an esker. The hydraulic properties varied between $8{\cdot}10^{-7}$ and $7{\cdot}10^{-5}$ m/s in the sand till areas and $4{\cdot}10^{-5}$ m/s and $2{\cdot}10^{-4}$ m/s on the edge of the glaciofluvial deposits. The groundwater depth varies between 0.38 m and 2 m below the surface. We have chosen to measure at four different areas (A, B, C, D) that differ in their (hydro-)geology and where wells were available (see Table 3 and Figure 5).

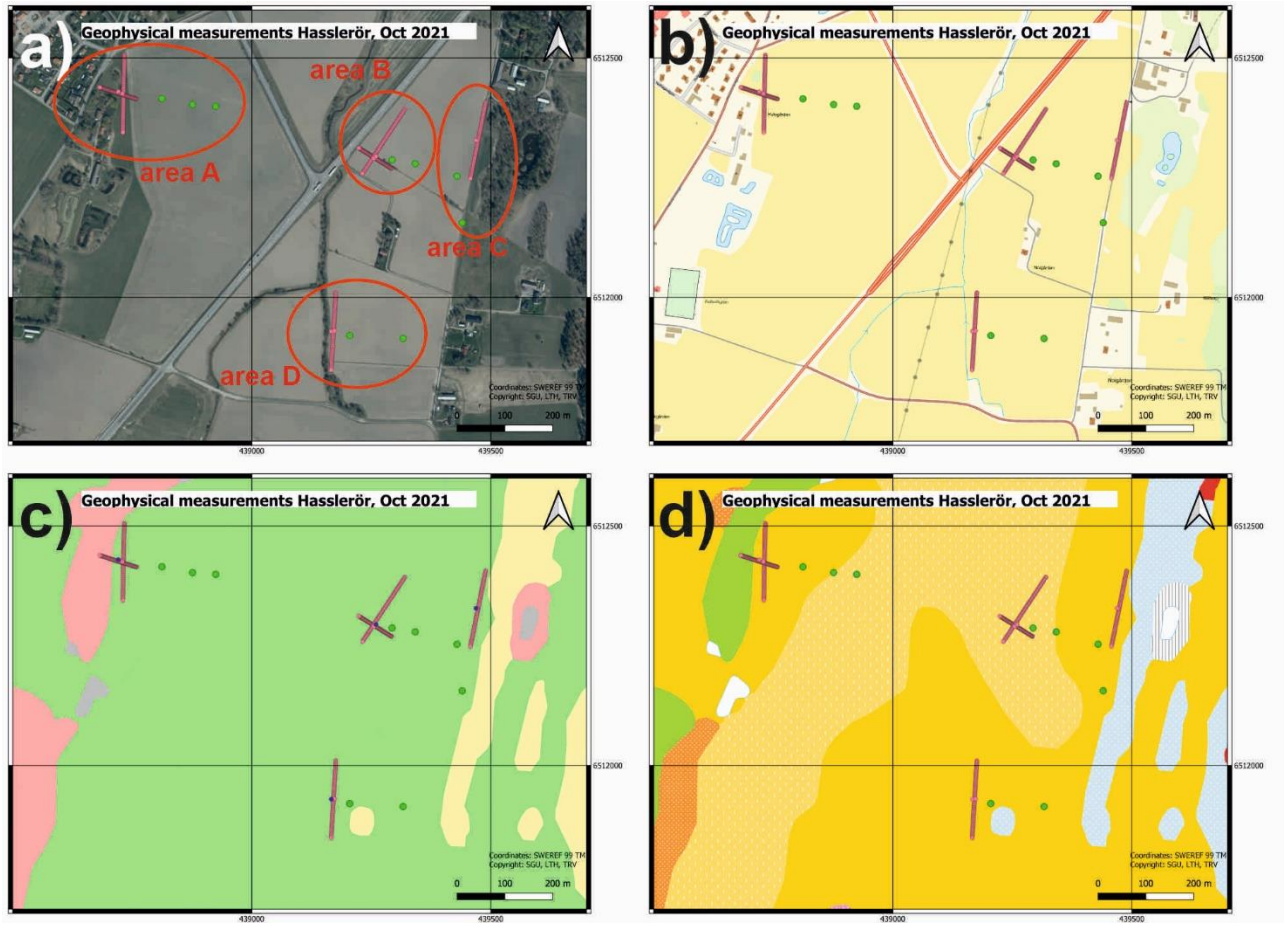

Figure 5: DCIP Profiles (red lines) and MRS soundings (green dots) for test site 2 – Hasslerör, plotted on a a) satellite map, b) topographic map, c) groundwater vulnerability map, d) soil characteristic map. Legend to c) and d) see Figure 4.

Table 3: Description of the test site 2 in Hasslerör.

Area	Well	Hydraulic Conductivity *K*	GW depth (Oct 2021)	Description	Comment
A	21019GW	$4*10^{-5}$ m/s (slug test), grain size analysis: $2\text{-}7*10^{-4}$ m/s	-2.00m	Post glacial deposits, saGr (sandy gravel), large esker	No power lines but close to houses and closer to train traffic
B	21007GW		-1.18m	Glacial clay	Much clay, close to power lines
C	21051GW	$2*10^{-5}$ m/s (slug test),	-0.91m	Glacial clay, SaTi (sand till)	Thinner clay layer than in B overlaying sand, electrical fence close by

D	21023GW		-0.38m	Glacial clay	Close to power line,

Altogether 6 DCIP profiles were measured in October 2021. Two of the profiles were measured with a shorter electrode distance (a = 1m) and a length of 81m, four of the profiles were 162m long with an electrode distance of a = 2m. More information can be found in Table 4.

In November 2021 also MRS measurements were done (green dots in Figure 5). Unfortunately, the noise contamination from multiple sources, including the highway, the nearby village, transformer and, additionally, a geomagnetic storm during acquisition has hindered a sufficient data quality. Hence, no useful results could be obtained and shown here.

Table 4: DCIP profile parameter for test site 2 - Hasslerör.

Area	Name of profile	Profile length [m]	Electrode distance [m]	Crosses well (at …profile m)
A	Site A - Profile L	162	2	21019GW (at 80 m)
A	Site A - Profile S	81	1	21019GW (at 41 m)
B	Site B - Profile S	81	1	21007GW (at 45 m)
B	Site B - Profile L	162	2	21007GW (at 120 m)
C	Site C	162	2	21051GW (at 81 m)
D	Site D	162	2	21023GW (at 81 m)

Test site 3: Mjölkalånga

The main requirement for test site 3 was a minimum of electromagnetic noise since test sites 1 and 2 that were already surveyed and evaluated were severe affected from anthropogenic noise. Here, no actual infrastructure construction is planned. Instead, earlier geophysical measurement results were available and provided by the Hässleholm municipality and WSP AB. Since no hydrological information could be found, the consultant company NIRAS was commissioned to conduct measurements with the hydraulic profiling tool (HPT) and slug tests at six drilling spots along two of the measured profiles. Four profiles were measured with DCIP and MRS in April 2022 (Figure 6). More than 30 MRS soundings were done along the four DCIP profiles (see attachment: report from Aarhus University). In addition to the field work, several soil samples from the first meter were taken from 9 different spots along all profiles (see also Figure 7).

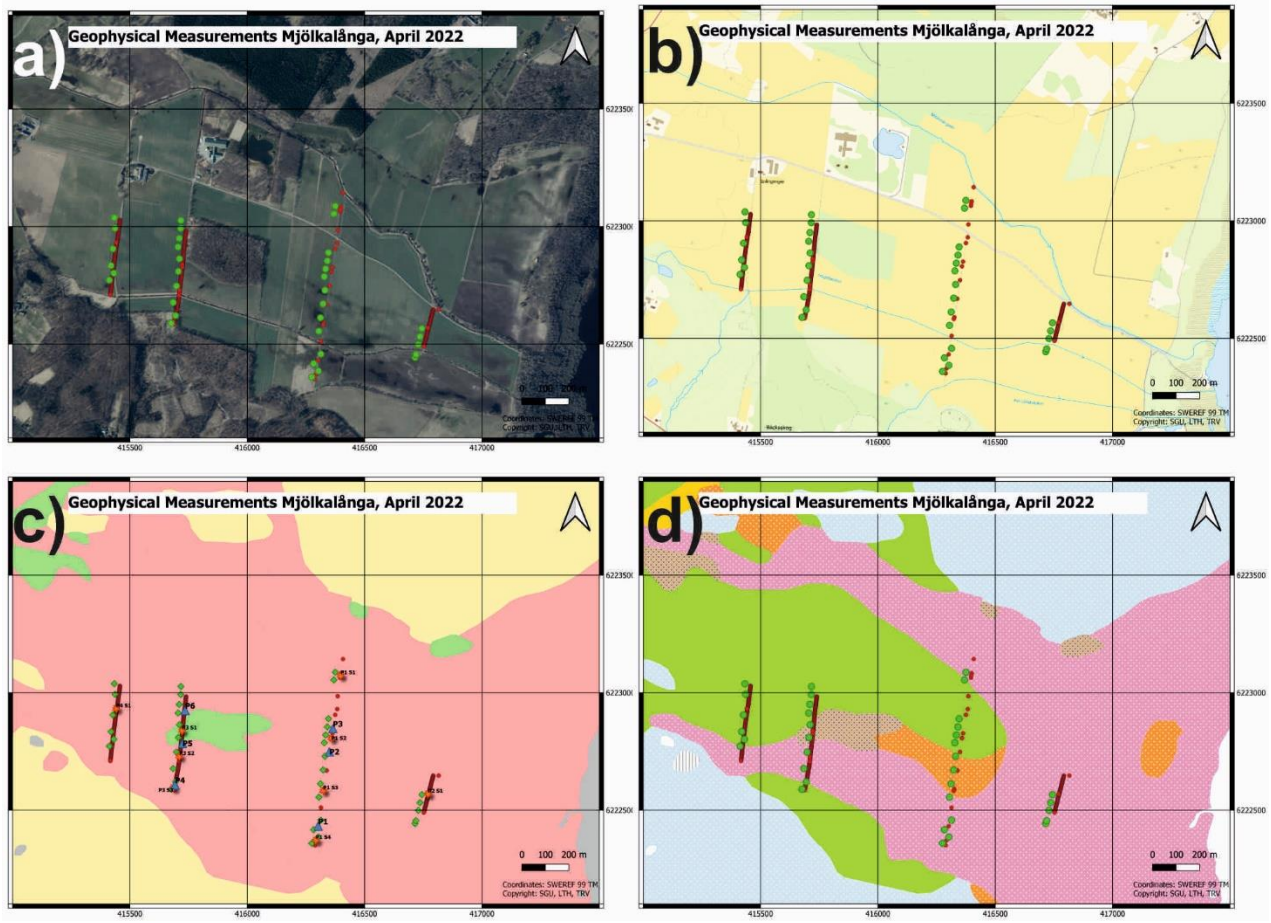

Figure 6: DCIP Profiles (red lines) and MRS soundings (green dots) for test site 3 – Mjölkalånga, plotted on a a) satellite map, b) topographic map, c) groundwater vulnerability map, d) soil characteristic map. Legend to c) and d) see Figure 4.

Table 5: DCIP profile parameter for test site 3 - Mjölkalånga.

Name of profile	Profile length [m]	Electrode distance [m]	comment
Profile 1	802	2	Gap data between 190m and 197m (road); measured in two days in roll along (9 parts)
Profile 2	162	2	
Profile 3	402	2	Measured in roll along (4 parts)
Profile 4	322	2	Measured in roll along (3 parts)

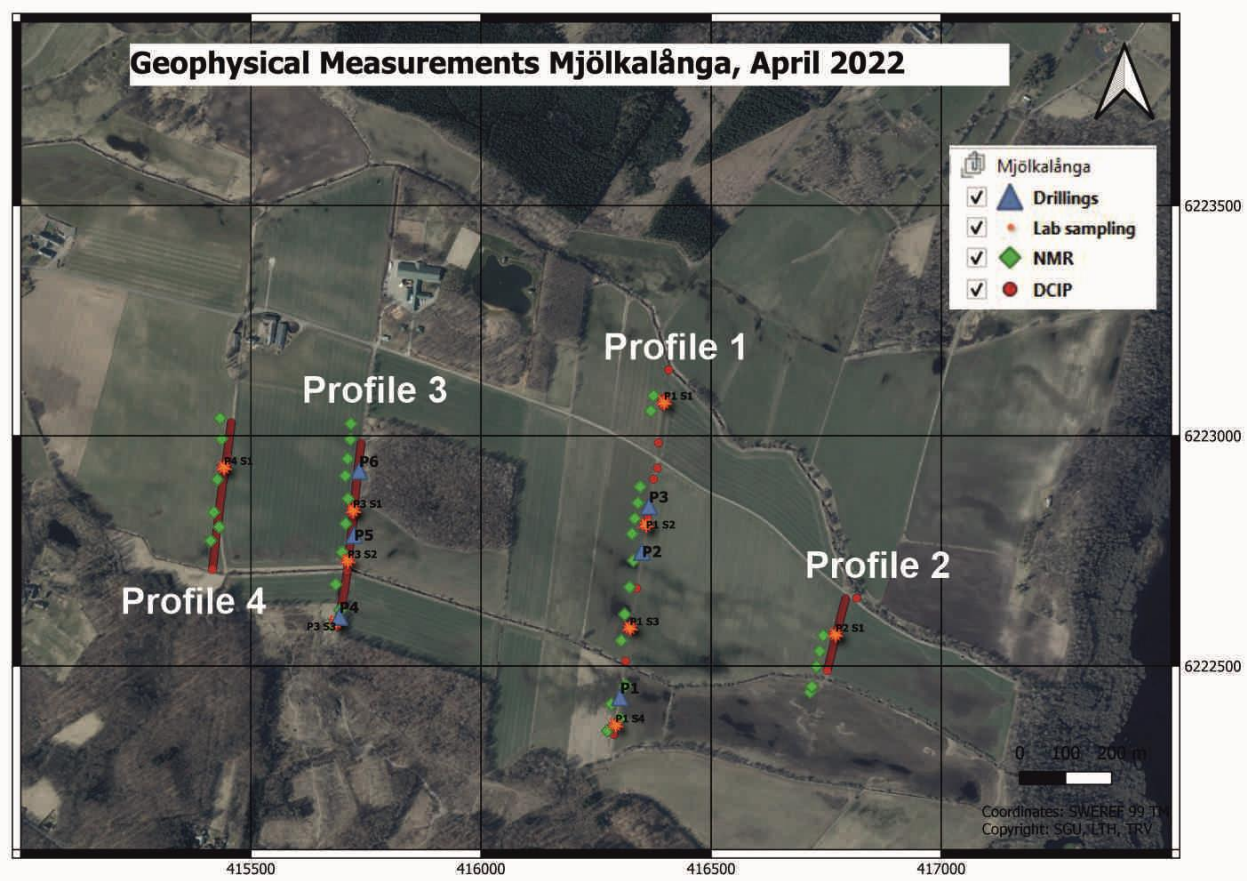

Figure 7: Detailed overview about all measurements in Mjölkalånga. Red dots: DCIP profiles; green squares: MRS soundings; blue triangles: Drilling spots; orange stars: Lab sampling points.

Results & Discussion

Due to the large number of data, only the apparent ("raw") data will be shown for all measured profiles. The inversion results will be only displayed for selected profiles (4 for each test site) in the report. The MRS results are shown for test site 1 (Börringe) and 3 (Mjölkalånga) but not for test site 2 (Hasslerör) since the data was too noisy for useful MRS interpretation. For test site 1 the MRS data quality was also low due to the presence of the large powerline subparallel to the highway that has contaminated most of the measurements but some modest data in the peat area could be obtained and shown here in the report. Detailed information about the MRS measurements can be also found in the two attached reports.

The HPT and slug test results are shown for test site 3 since they were only conducted there.

Test site 1: Börringe/Svedala

In Figure 8 and Figure 9, the apparent resistivity and phase data from all profiles at area A and B are displayed. In general, the apparent resistivity looks quite homogeneous. Only between 100m and 120m at the A148P# – profiles show a decrease in the values. That correlates with the higher chargeability zone in the apparent chargeability plots. The cross profile A148Px correlates well with the rest of the A148P# profiles. Even though profile A67P1 is a bit further away, it shows the same range of values and the anomaly at the same spot.

At area B a clear layering in the apparent resistivity data can be seen. On top is a layer of lower resistivities whereas in depth the resistivities increase. The chargeability data are very small, but a slight trend can be observed. In general, the values on top are even smaller and close to zero than in greater depths.

The data quality of the profiles is good and potential noise from the power lines could be filtered during the DCIP processing.

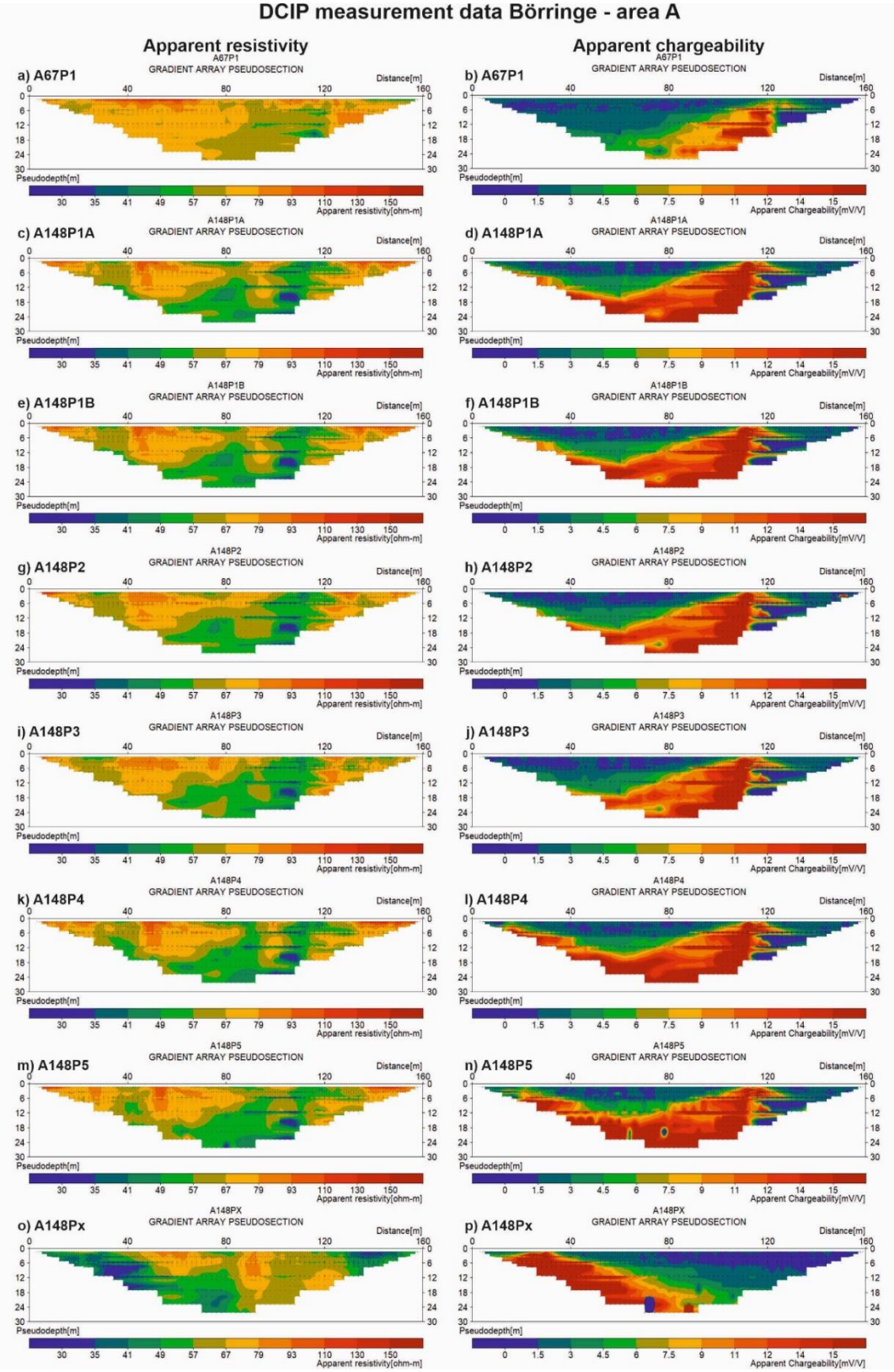

Figure 8: Apparent resistivity (to the left) and chargeability sections (to the right) for all measured DCIP profiles at area A in Börringe.

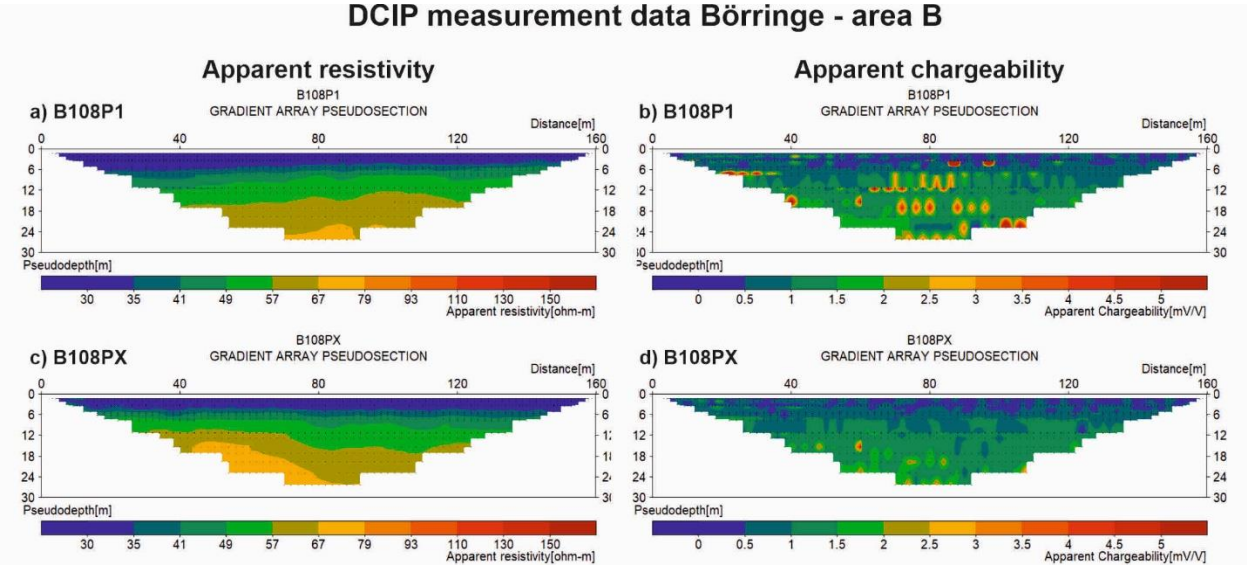

Figure 9: Apparent resistivity (to the left) and chargeability sections (to the right) for all measured DCIP profiles at area B in Börringe. Note: the chargeability colour scale is slightly different to the scales at area A since the signal were smaller.

In Figure 10, the inversion results for the four profiles A67P1 (a), A148P1a (b), B108P1 (c) and A148P1x (d) can be seen. In addition to the resistivity ρ (top) and phase ϕ (middle)- that is the equivalent of the apparent chargeabilities from the raw data -, also the calculated intrinsic permeability *k* is displayed (bottom section).

In the first 1-2m at profile A67P1 (a), a higher resistivity layer (200 Ωm) can be seen. Below that, a lower resistivity zone (50 Ωm) with a thickness of approx. 4 – 5 m can be found. Below 6 m depth, the resistivities increase again. An anomaly is visible at profile meter 128 m. Most likely, that has some anthropogenic causes (buried pipe?) and should not be considered in the interpretation. The highest phases values can be found in the first 1-2 m and show values up to 20 mrad. Below that top layer, the phase values decrease with depth. The calculated intrinsic permeabilities *k* show values around 1-5*10^{-12} m^2 in the upper few meters. In greater depths, the intrinsic permeability increases up to 5*10^{-11} m^2. According to the hydraulic conductivities values from 2017 in 0.9 m depth (TRV 2020a, K=1.9*10^{-6} m/s), the expected intrinsic permeabilities values at profile meter 64 m should be around 10^{-13} m^2 (see eq. 2).

Profile A148P1a (b) shows the same tendency and distribution as profile A67P1. Based on the data from 2017, the hydraulic conductivity was 2.4*10^{-7} m/s in 2-4 m depth (and at profile meter 21 m) which can be transformed to intrinsic permeability values of approx. *k* = 2.4*10^{-14} m^2 (eq. 2). In our DCIP – *k* section we find at this spot intrinsic permeability values of approx. 1*10^{-13} m^2.

At area B, the resistivity distribution for profile B108P1 (c) is different than for area A. Here, a thick layer (5-6 m) of low resistivities can be seen over the entire section. That corresponds to the clay layer in that area. Below that, the resistivities increases with depth. In phase, the

lowest values can be found on top. In general, the phase values increase with depth, only in the western part a thick low phase zone is visible until 12 m depth. For profile B108P1 (c) the calculated intrinsic permeabilities *k* of $9*10^{-14}$ m^2 from DCIP are much smaller than reported by Trafikverket with *k*=$2.1*10^{-16}$ m^2 (K=$2.1*10^{-9}$ m/s) at profile meter 81 m and in 7.5 m depth.

The resistivity and phase properties (and therewith the intrinsic permeability) for profile A148Px (d) changes along the profile. Some low resistivity lenses (10-20 Ωm) show up in 2-3 m depth. They are embedded in a higher resistivity area with values up to 200 Ωm. The highest phase values with values above 20 mrad can be seen on the west side of the profile (to the left). Towards East the phase values decrease. Based on the phase distribution, the intrinsic permeability is lower in the western part than in the East and reaches from $<10^{-13}$ m^2 to $5*10^{-12}$ m^2. At profile meter 78 m, Trafikverket reports 2017 a hydraulic conductivity value of K = $1.7*10^{-7}$ m/s in 2-4 m depth which corresponds to an approximated intrinsic permeability of $1.7*10^{-14}$ m^2.

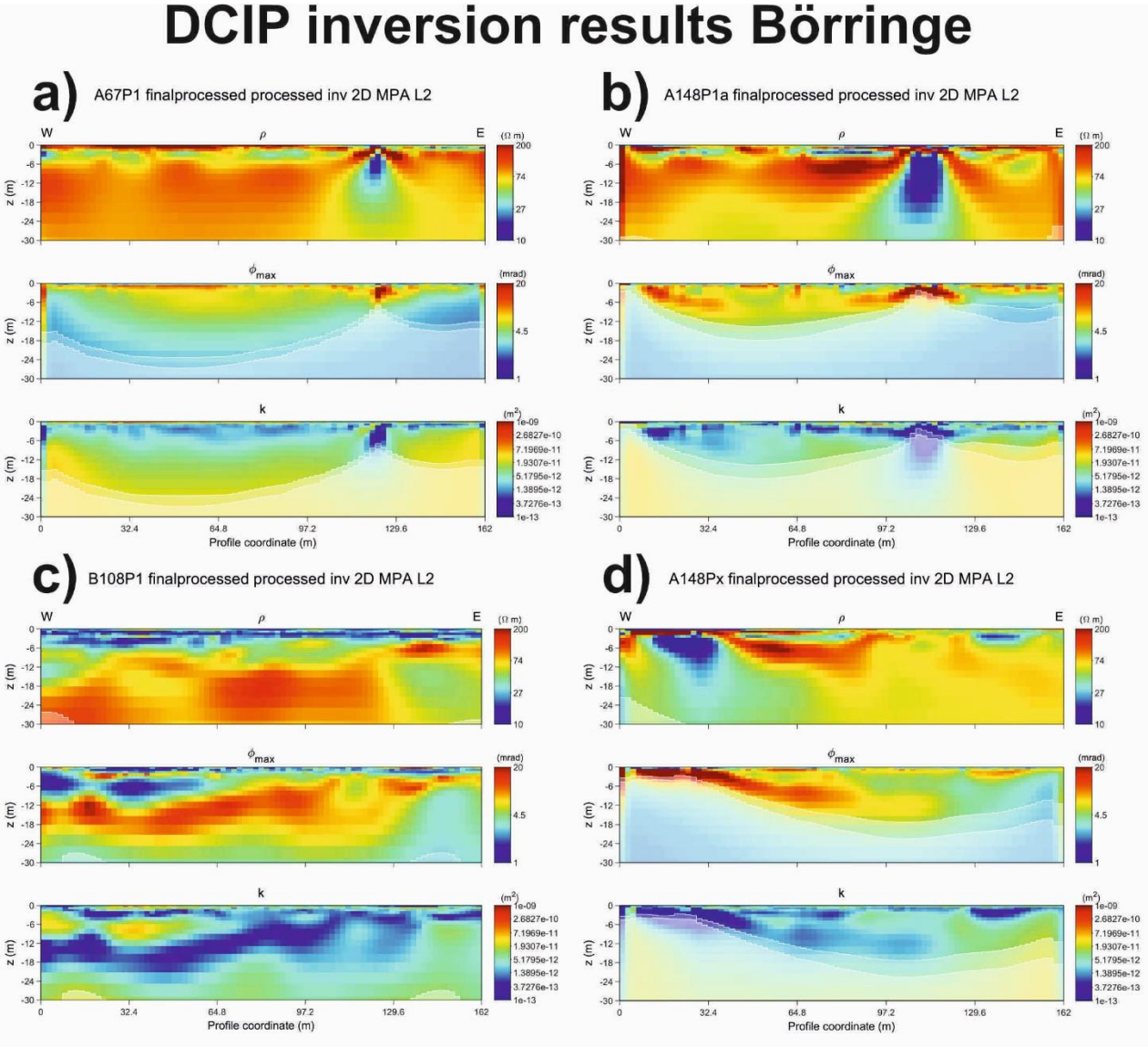

Figure 10: Inversion results for profiles A67P1 (a), A148P1a (b), B108P1 (c) and P148Px (d). For each profile it is shown from top to bottom: resistivity ρ – phase ϕ - calculated intrinsic permeability k. The anomalies at profile meter 128 (A67P1) resp. 110m (A148P1a) is, most likely, anthropogenic noise (buried pipe?) and should not be considered in the interpretation.

Even though the MRS data is strongly affected by noise and the resulting signals were small, the cross plot of the measured sounding can be seen in Figure 11 (visualised as juxtaposition of the soundings). Due to the high noise level an interpretation is difficult, however the higher water content in the peat area (area C) can be seen close to the surface at S06 (550 m). That correlates with higher relaxation times.

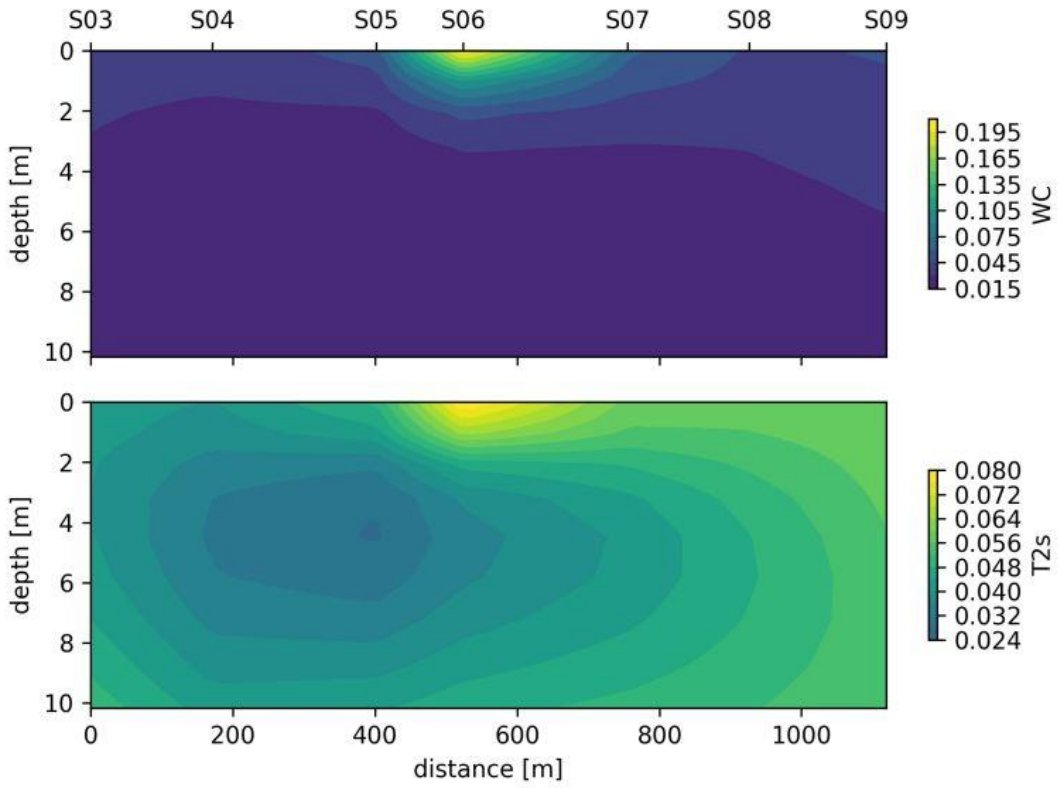

Figure 11: MRS results for test site 1. The cross section combines the measured soundings (visualised as juxtaposition of the soundings – see Figure 3 green dots).

Test site 2: Hasslerör/Mariestad

The DCIP raw data for all profiles in Hasslerör is displayed in Figure 12. Again, the DCIP data quality is good. In general, a low resistivity zone of varying thickness on top of higher resistivities can be seen in all resistivity sections (to the left). Only at site A - profile S (c, d) the transition from the glacial clay to the post glacial deposits (sandy gravel, large esker) is notable. The apparent chargeabilities are small and increase slightly with depth. Only site A - profile L (b) shows higher chargeability values closer to the surface.

In Figure 13 the inversion results for four selected profiles are shown. At all profiles, a low resistive top layer can be found with varying thickness. At site D, the thickness is largest with approx. 7-8 m. The low resistivity layer corresponds to the glacial clay in that area. In depth, the resistivities increase. The highest resistivities could be found at site C with values up to 10 000 Ωm. In all phase sections a thin high phase layer (1-2m) can be seen. Below that, the phase decreases before they increase again in 4-6 m depth. Only at site C, the right part of the profile shows a continuous low phase zone even until greater depths. The intrinsic permeability distribution varies significantly and depends on the depth. Whereas very low intrinsic permeabilities can be seen at site A - profile L (down to 10^{-13} m^2), the values for profile site B, C and D are much higher in general (up to 10^{-10} m^2). The reported hydraulic conductivity at site A (profile meter 80 m and in approx. 5 m depth) is $4*10^{-5}$ m/s (TRV 2020b), which converts to an

intrinsic permeability of $4*10^{-12}$ m^2. That corresponds well with the measure DCIP intrinsic permeability of approx. $4*10^{-12}$ m^2. At area C, where hydraulic conductivities values of $2*10^{-5}$ m/s are reported, respectively intrinsic permeabilities of $2*10^{-12}$ m^2, the intrinsic permeability values from DCIP measurements around $2*10^{-10}$ m^2 is much smaller.

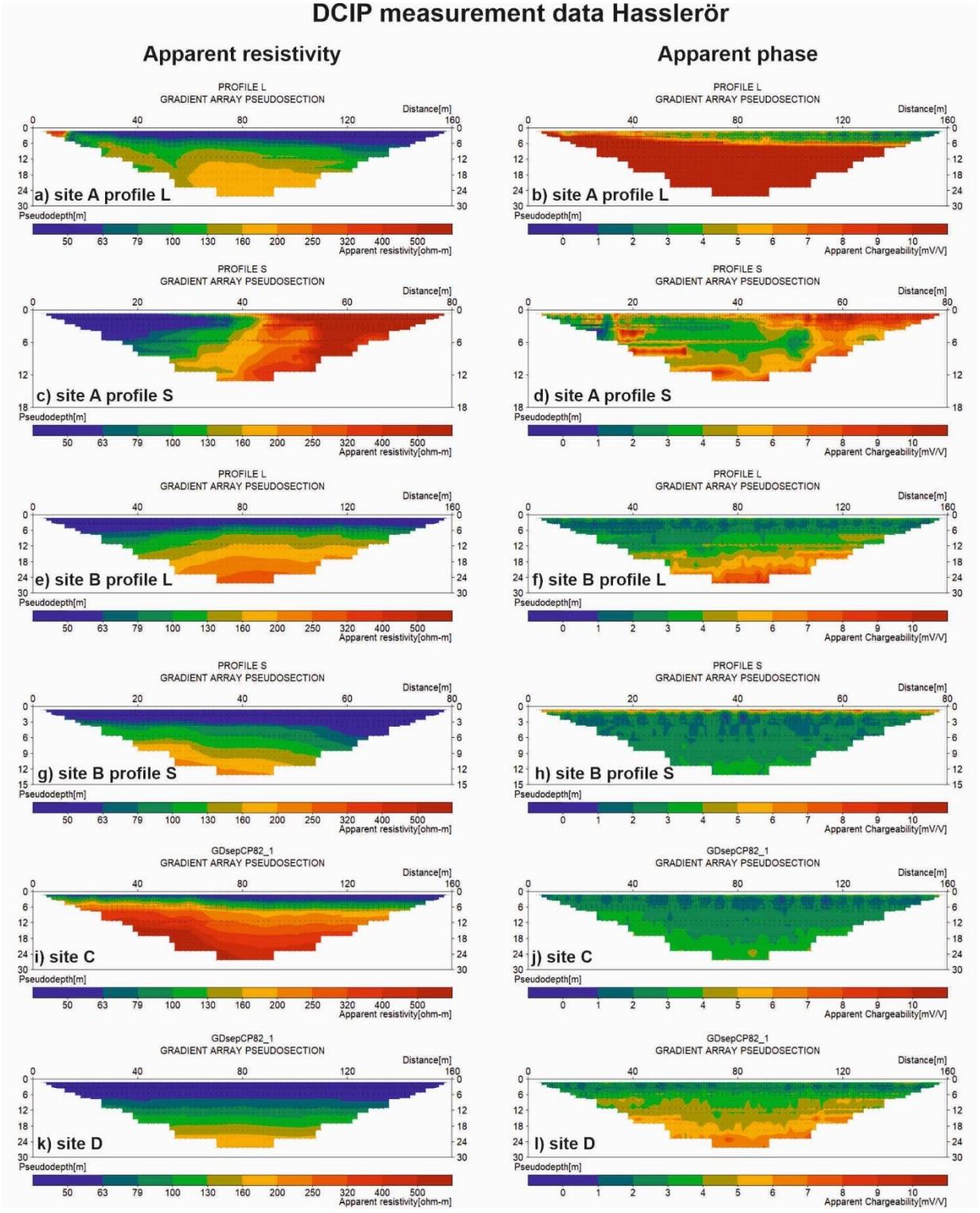

Figure 12: Apparent resistivity (to the left) and chargeability sections (to the right) for all measured DCIP profiles in Hasslerör.

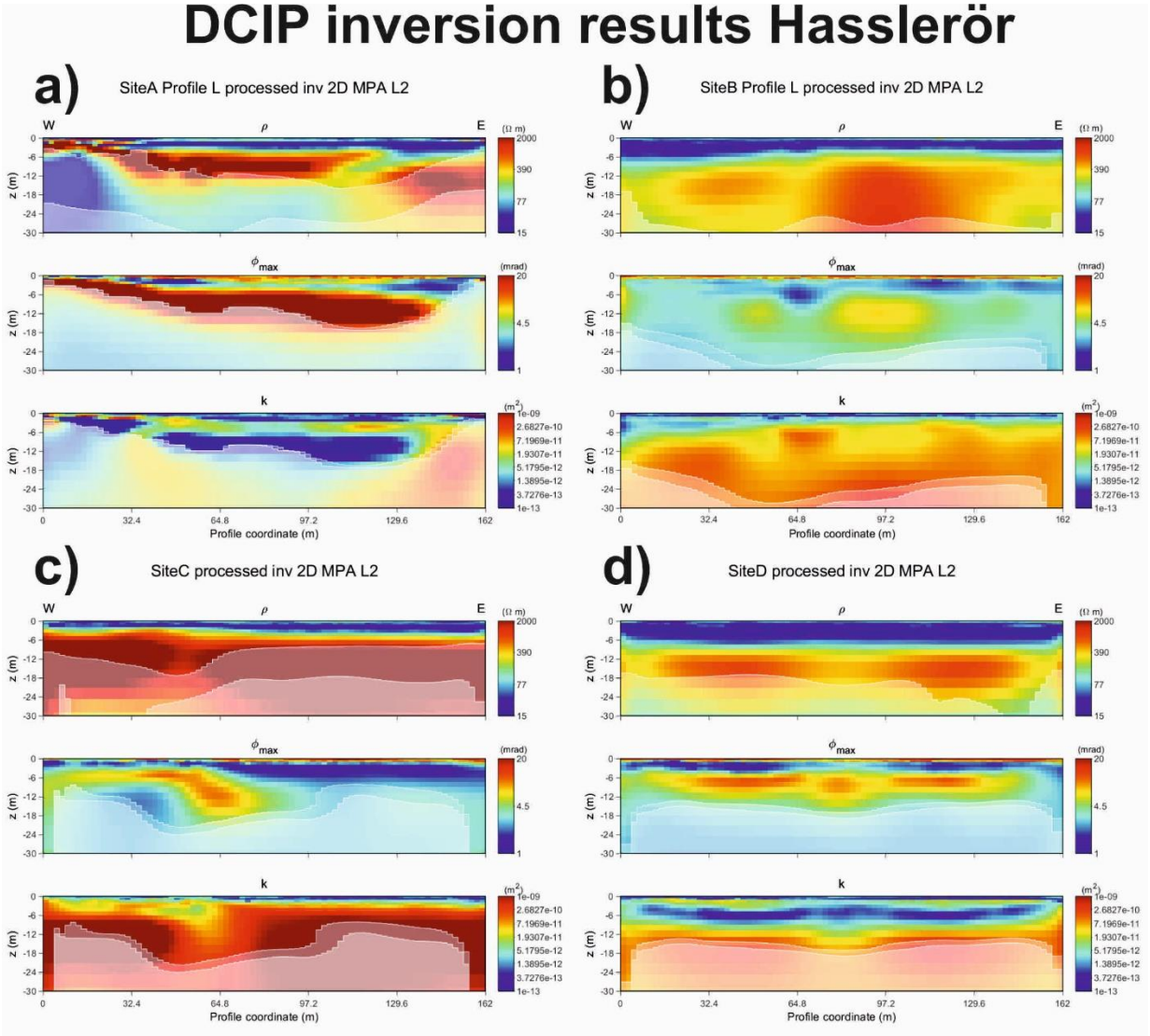

Figure 13: Inversion results for 4 selected profiles in Hasslerör: a) Site A profile L; b) Site B profile L; c) Site C; d) Site C. Top left: site A profile L; top right: site B profile L; bottom left: site C; bottom right: site D. For each profile it is shown from top to bottom: resistivity ρ – phase ϕ - calculated intrinsic permeability k.

Test site 3: Mjölkalånga

The DCIP raw data for the four profiles in Mjölkalånga are shown in Figure 14. The data quality is very good for this site and only minor processing was needed. Profile 1 covered a long distance (802 m) and several geological units, which can be seen in the apparent resistivity section. A higher resistive layer can be observed between 70 m and 400 m. Between 400 and approx. 700 m, the lower resistivities reaches the surface before another high resistive zone shows up behind 700 profile meters. The anomaly at 520 m is probably of anthropogenic origin

(buried pipe?) and should not be considered in the interpretation. The other three profiles are also characterised by a higher resistive layer. Below that, the resistivities decrease. The chargeability values are usually small. Slightly higher values could be found at profile 4.

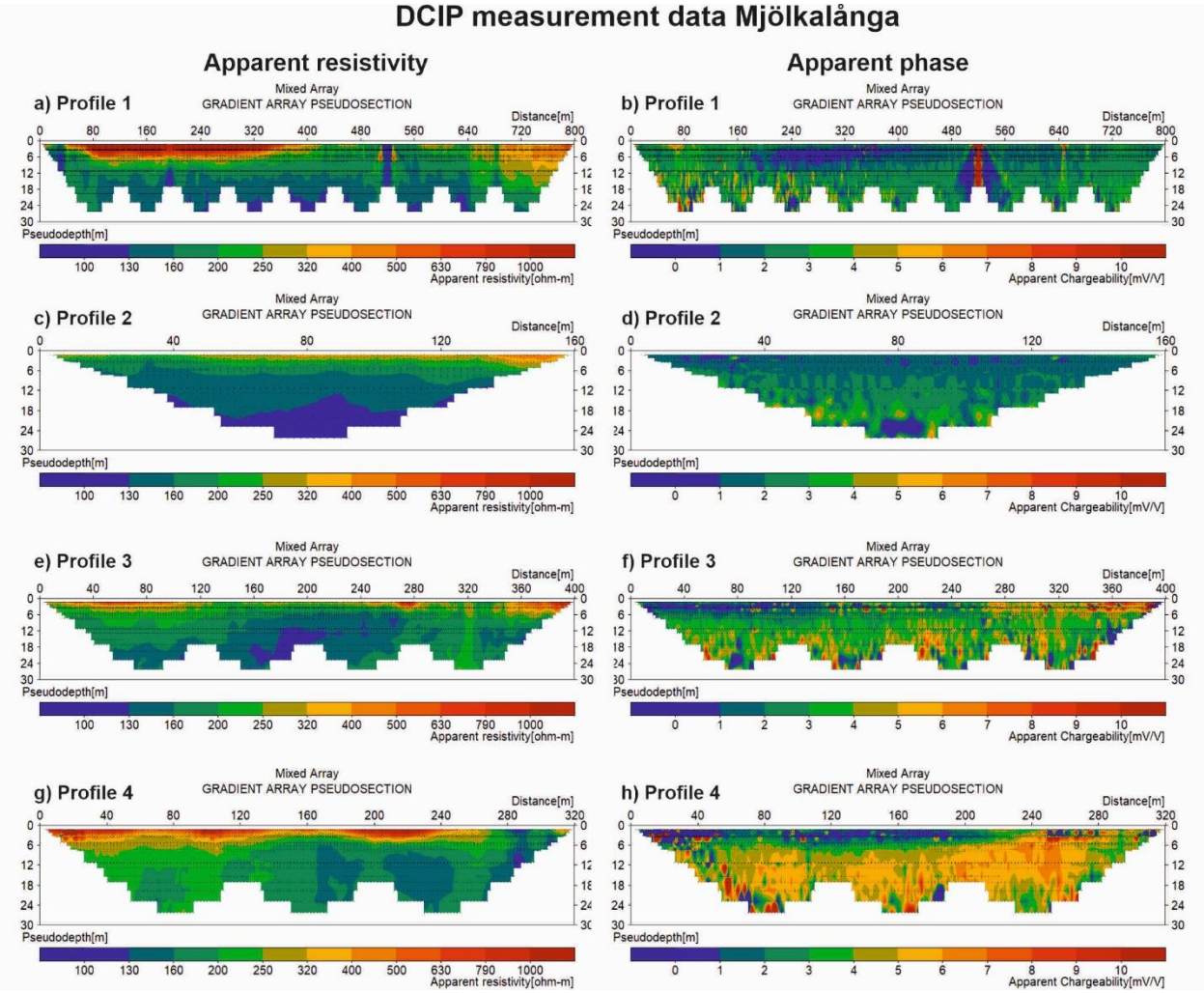

Figure 14: Apparent resistivity (to the left) and chargeability sections (to the right) for the four measured DCIP profiles in Mjölkalånga.

The DCIP inversion results for the four profiles can be found in Figure 15. Different layers of lower and higher resistivities alternate along the profile. Mostly, a higher resistivity layer can be found on top. The thickness of this layer varies between and along the profiles. With depth, the resistivities decrease. Only for profile 3 a higher resistivity zone can be also detected in depth (below 12 m) between 240 m and 400 m. Different layer can be also seen in the phase sections. On top, the phase values are small. Below that a thick layer (up to 10 m) of higher phases could be measured. The intrinsic permeability calculations show values between 10^{-14} and 10^{-8} m^2.

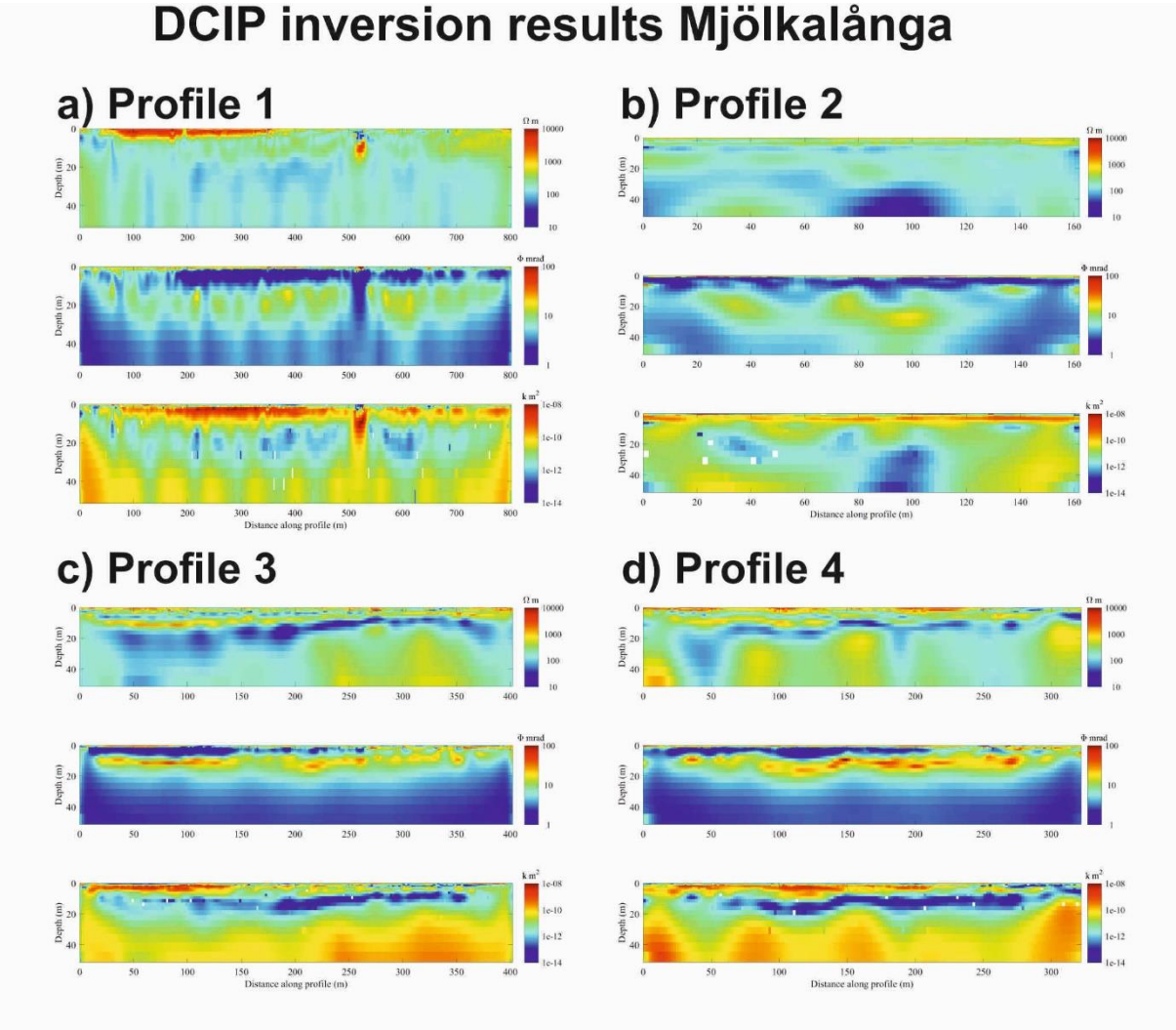

Figure 15: Inversion results for the four profiles in Mjölkalånga. a) Profile 1; b) Profile 2; c) Profile 3; d) Profile 4. For each profile it is shown from top to bottom: resistivity ρ – phase ϕ – calculated intrinsic permeability k.

The inversion results for the MRS sounding can be seen in Figure 16. The areas between the soundings are interpolated. For each profile the water content section (WC) and the relaxation time T2* section is shown. The ticks on top of each section mark the soundings, the ticks on the bottom line of each section mark the distance. In all water content sections can be seen that the water content is maximal close to the surface. The thickness of the higher-water-content layer increases from West to East and reaches its maximum with > 5 m at profile 2 (closest to the lake). The relaxation time increases with depth for all profiles. The changes in water content and relaxation time along the respective profiles are only minor. More detailed data can be found in the attached report from Aarhus University.

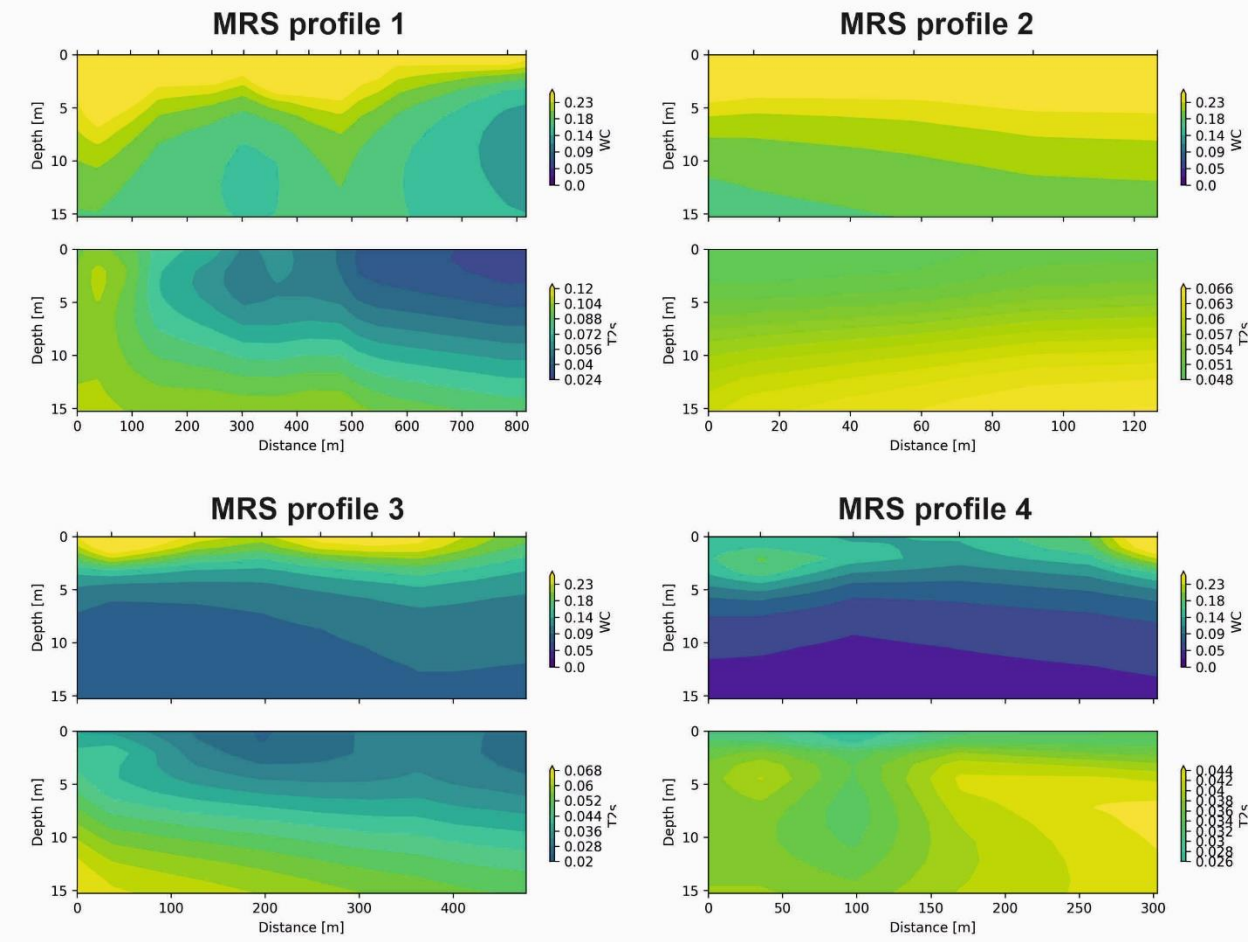

Figure 16: MRS inversion results for all soundings at the four profiles. For each profile the water content section (WC) and the relaxation time T2 section is shown. The ticks on top of each section mark the soundings, the ticks on the bottom line of each section mark the distance.*

At test site 3 also hydraulic testing with the hydraulic profiling tool and slug tests were conducted by the company NIRAS. Selected parts of the results can be found in Figure 17. Boreholes P1, P2 and P3 were drilled on profile 1, boreholes P4, P5 and P6 on profile 3. The variation in the estimated hydraulic conductivity from HPT is small for the first three boreholes (top row). Occasional peaks to lower K-values occur. At P4, P5 and P6 layers with different estimated K values can be recognized.

The hydraulic conductivity from the slug test agrees with the HPT data to some extent, but for P1 an offset was measured. For the other boreholes both values are mostly very similar, but for profile 3 an offset with an approximate factor of two is observed for the shallowest slug test. Furthermore, for P5 a large offset is evident for the slug test result at 13m depth. In the bottom row, the EC log is shown together with the slug test results. Despite the first 2 meters, the variation in the EC is small. In tendency there is an increase of electrical conductivity with depth. The general trend between the EC log and the resistivity from the DCIP measurements is the same.

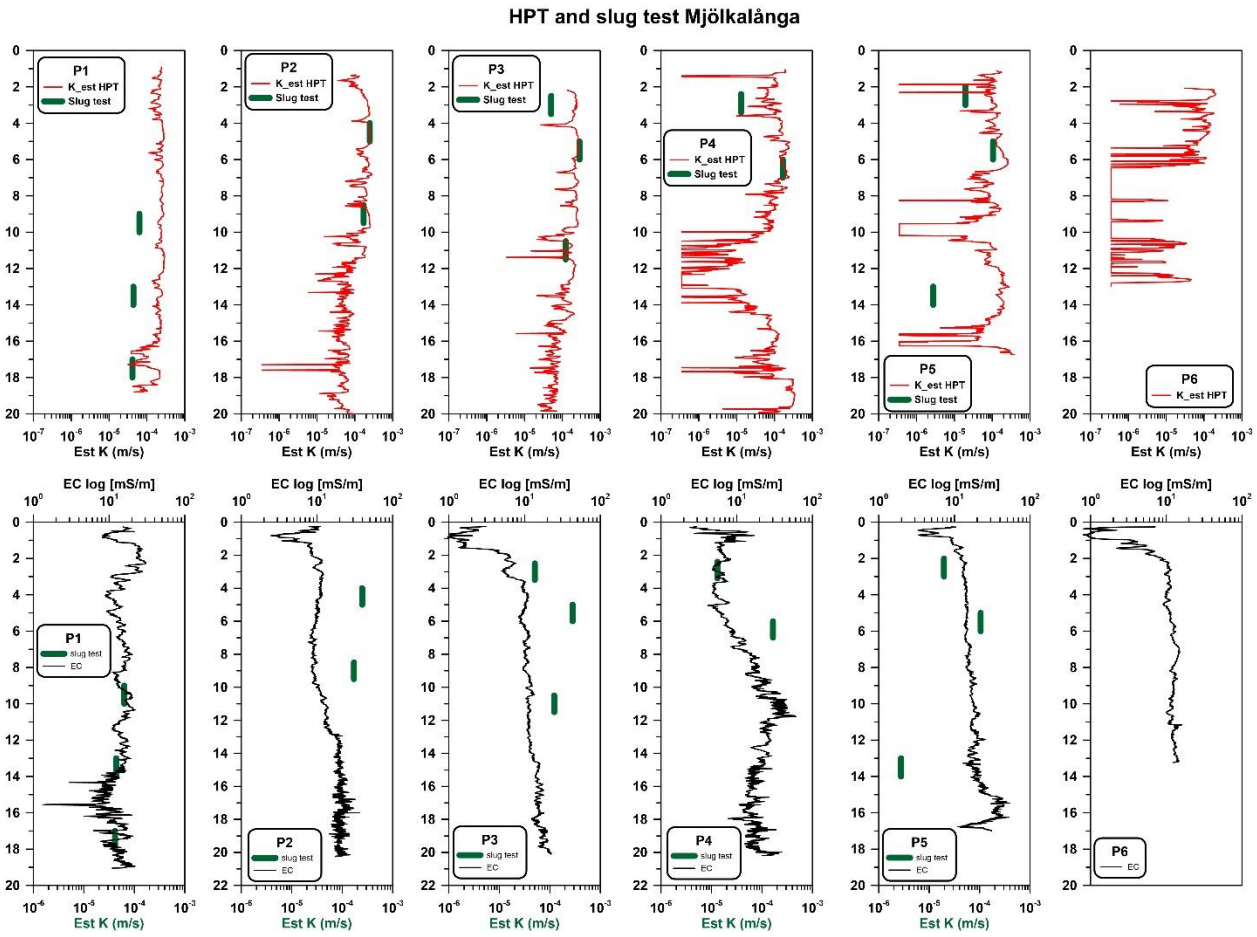

Figure 17: HPT and slug test results for the six borehole measurements at Mjölkalånga. Top row: Estimated hydraulic conductivity (K) from HPT (red line) and measured hydraulic conductivity from slug tests (green); bottom row: EC log (black line) and slug test results (green). Note: In borehole 6 (P6) no slug tests could be conducted. Boreholes P1, P2 and P3 were drilled on profile 1, boreholes P4, P5 and P6 on profile 3.

The comparison between the hydraulic conductivity (HPT & slug tests), intrinsic permeability estimated from the DCIP results and water content and relaxation time from the MRS measurements for profiles 1 and 3 are shown in Figure 18 and Figure 19. In borehole P1 (Figure 18) the estimated hydraulic conductivity from HPT seems to be constantly high with the investigated depth. For P2 and P3 a general trend of decreasing hydraulic conductivities with depth can be seen. The intrinsic permeability distribution from DCIP follows the same trend. With increasing depth, the intrinsic permeability decreases. In Figure 20 the closeup for the boreholes at profile 1 can be seen (top row). Both slug test data and HPT fit remarkably well in their tendential course with the DCIP – *k* values.

The general trend of lower hydraulic conductivities with depth is indicated in the water content distribution in the MRS data. Similarly to the DCIP results, the water content drops significantly after approximately 10 metres depending on location. The T2* parameter in the top 10 metres

of profile 1 shows a reduction in pore space from south to north, coincident with the reduced intrinsic permeability estimates from DCIP.

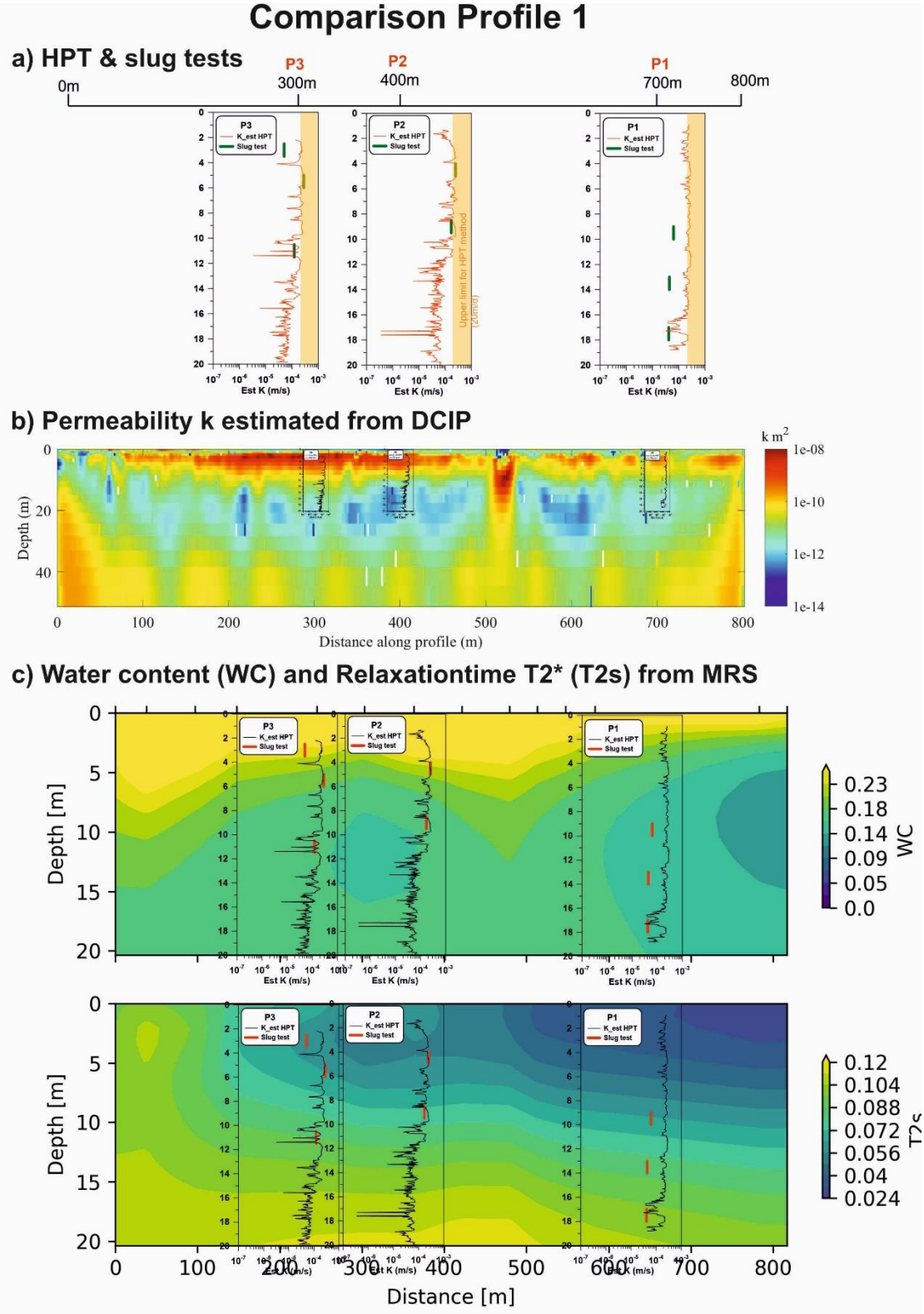

Figure 18: Comparison between the hydraulic conductivity from HPT and slug tests (a), intrinsic permeability k estimated from DCIP results (b) and water content distribution (WC) and relaxation time (T2s) from MRS measurements for profile 1 (c). Note: the MRS section starts 60m behind the DCIP profile.

For profile 3, the comparison is shown in Figure 19 (with a closeup in Figure 20). For borehole P6, the HPT results show higher hydraulic conductivities in the first 6 meters with a decrease at greater depths. That fits very well with the increasing intrinsic permeabilities from DCIP. In drilling P5, the deep HPT results do not fit with the DCIP results. Instead, the three slug test values in 2m, 6m and 13m depth can be linked to the DCIP intrinsic permeabilities. In P4 both the HPT and slug tests confirm the DCIP intrinsic permeabilities.

For the first 6 to 10 m the general trend of a decreasing water content with depth confirms the HPT and slug test results. In greater depths, no correlation can be found, likely due to resolution differences between the MRS and slug tests as well as changing mineralogy with depth. The T2* parameter is also proportional to porosity, not intrinsic permeability, without further non-linear transforms related to soil type.

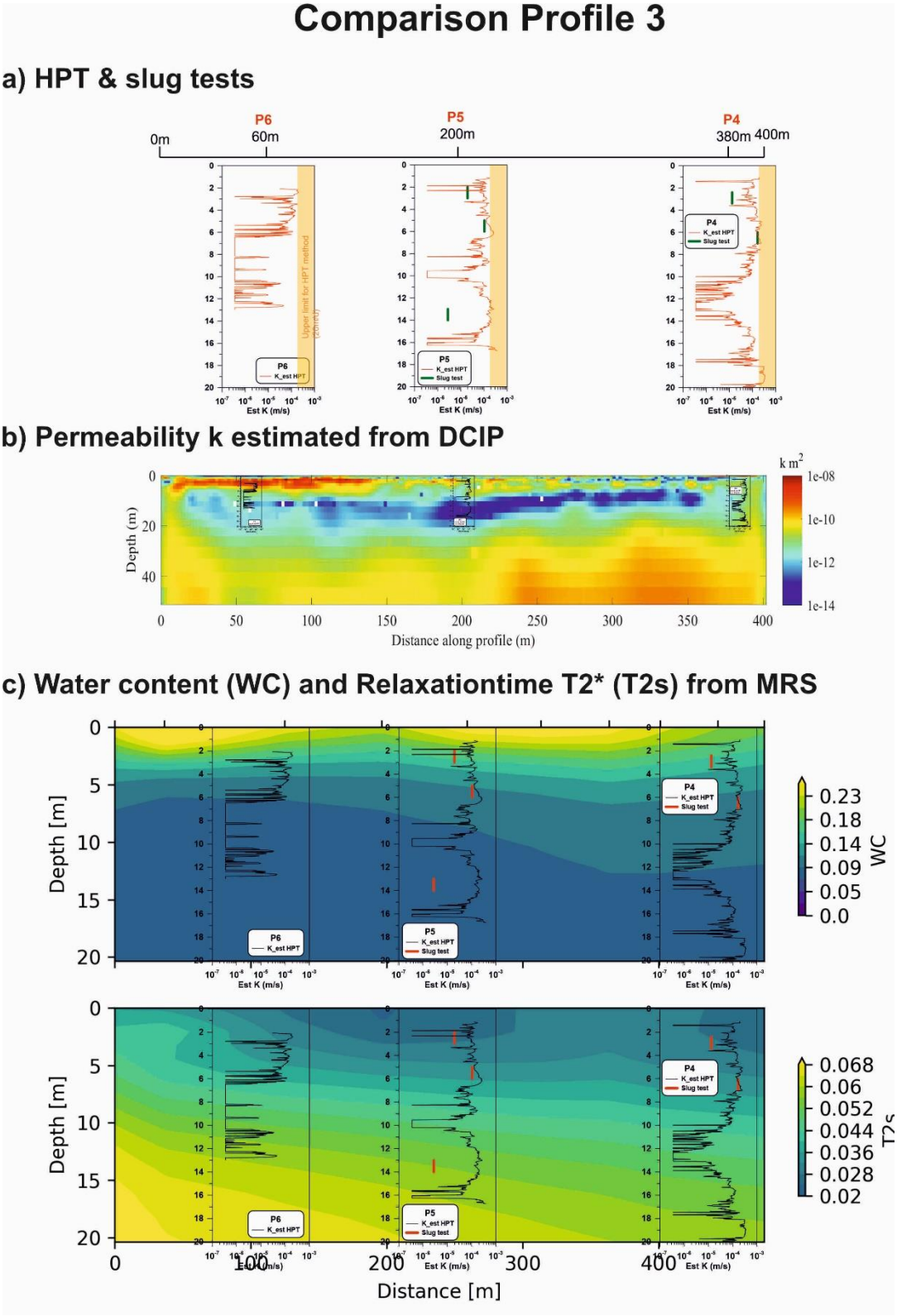

Figure 19: Comparison between the hydraulic conductivity from HPT and slug tests (a), intrinsic permeability k estimated from DCIP results (b) and water content distribution and relaxation

time from MRS measurements for profile 3 (c). Note: the MRS section starts 40m ahead of the DCIP profile.

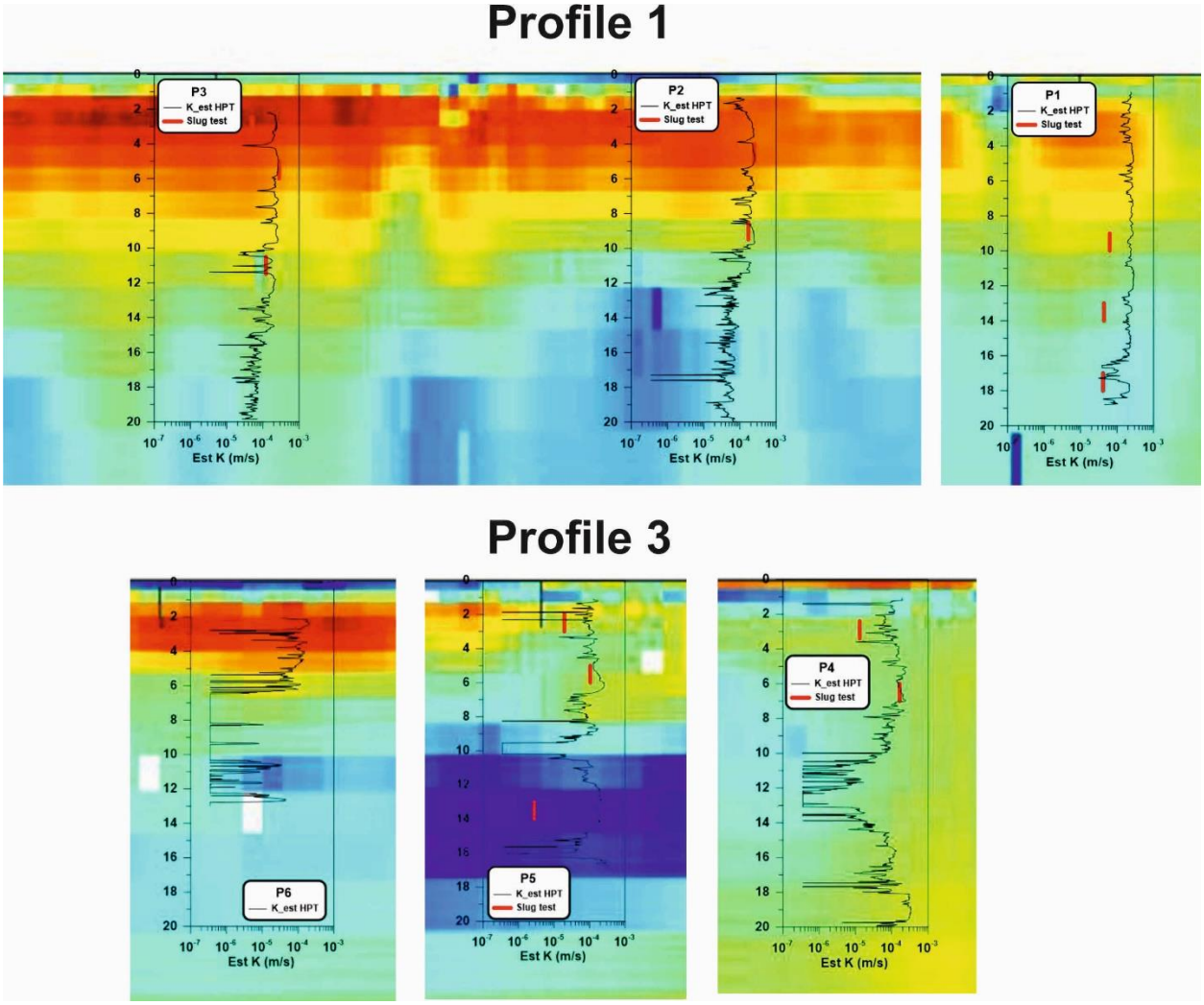

Figure 20: Closeup for the overlay of HPT/slug test hydraulic conductivity data and intrinsic permeability distribution from DCIP for all six boreholes (compare also Figure 18 and Figure 19).

Conclusion, evaluation & outlook

Comparing the geophysical results from DCIP and MRS measurements with the HPT and slug test results, a strong correlation can be seen within 1-2 decades in intrinsic permeability (Figure 21). However, the values are consistently higher for the DCIP *k* calculation compared to the slug test values.

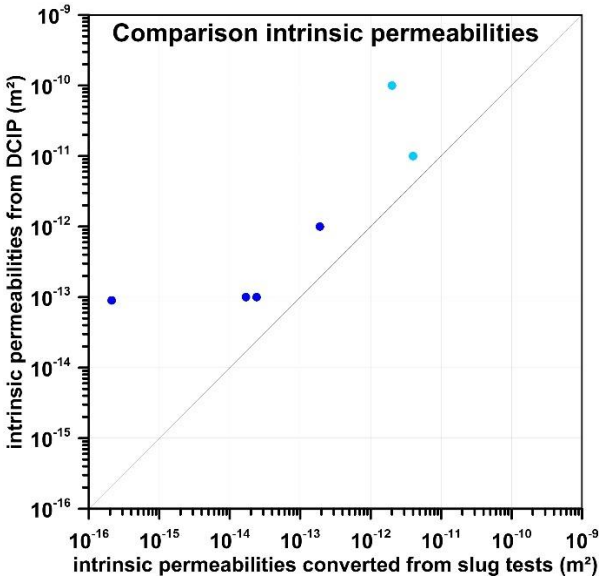

Figure 21: Comparison of intrinsic permeability for the first two test sites (Börringe- dark blue, Hasslerör - light blue) based on slug test data reported by Trafikverket in 2017 (TRV 2020a, TRV 2020b). The intrinsic permeability on the x-axis is converted from hydraulic conductivity via eq. 2.

In Figure 22, the cross plot from the slug tests (x-axis in m/s) at test site 3 in Mjölkalånga (profile 3) is shown together with the estimation of the hydraulic conductivity derived from DCIP intrinsic permeability (y-axis) with the new - still in the development - approach. Already at this stage, a better fit than in Figure 21 can be seen. Nevertheless, the aim of the ongoing research is to improve even that fit and adapt/test it on other test sites. That would significantly improve the estimation of the hydraulic conductivity respectively the intrinsic permeability and the prediction of pitfalls. In a potential continued research project, the next steps are further tests that should confirm the new relationship approach by, for example, using the methods in a borehole setup and at other geological settings.

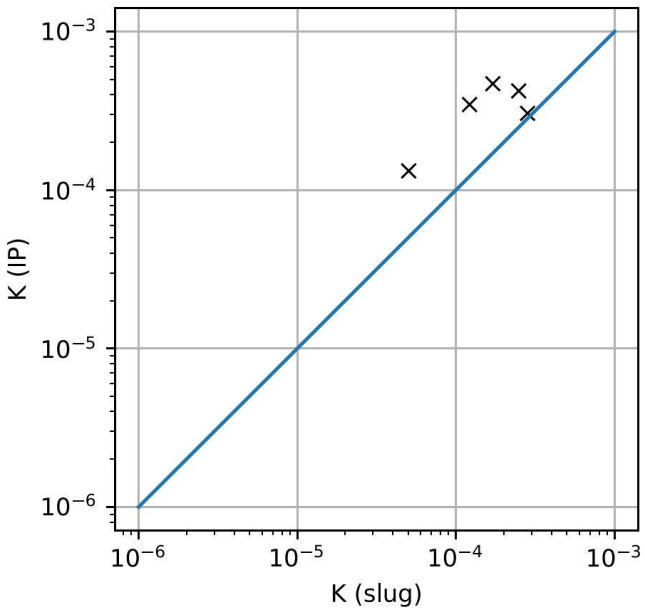

Figure 22: Cross plot of the hydraulic conductivity from slug tests (x-axis) and from the calculation based on the DCIP measurements (y-axis).

In general, the geophysical methods DCIP and MRS have the potential to reveal important hydraulic information of the underground. Our results are promising but need to get confirmed by further studies. The DCIP method could be applied all three test sites without restrictions. By using, for example, intelligent measurement setup (e.g., separated current and potential cables) and optimized measurement arrays, the data quality could be enhanced, and the measurement time decreased. Furthermore, thanks to new processing routines any potential anthropogenic noise could be filtered, and the resulting data quality was very good. The use of the DCIP method can be recommended at the above investigated kind of construction and test sites without reservation.

The MRS method was more affected by noise. For example, it was not possible to get sufficient data quality at test site 2 (Hasslerör). That data was not usable due to severe noise contamination from multiple sources, including the major highway, the nearby village, and a transformer station. At test site 1 (Börringe) the MRS data was severely hampered by electromagnetic noise from a variety of sources. For example, the presence of the large powerline subparallel to the highway contaminated most of the measurements. However, due to an improvement processing, it was still possible to obtain a usable line of data but due to the general low water content in that area (and the resulting low signals) an interpretation of the MRS data was difficult. In contrast, at test site 3 (Mjölkalånga) the (only minor) noise could be handled by the processing and the data quality was very good. Here, many sets of high-quality sounding data were obtained in a lateral density not previously acquired. Therefore, at sufficient noise-free sites, the MRS method can be highly recommended since it provides the

actual water content of the subsurface. At active construction sites or sites close to urban structures, the MRS method still suffers from the high noise and cannot be usefully applied.

Dissemination

During the project time we have attended national and international conferences and society meetings and have presented the project and results. Please find below an overview about the presentations.

2022, March: Annual conference of the German Geophysical Society (DGG) online/Munich, Germany. Abstract & Poster: *Geophysical mapping of aquifer properties in infrastructure projects using DCIP and MRS*

2022, May: Internal Engineering Geology/ Lund University seminar. Presentation: *Geophysical mapping of groundwater properties for transport infrastructure construction planning (DCIP/MRS)*

2022, June: International Induced Polarisation workshop, Annecy, France. Abstract & Poster: *Geophysical mapping of aquifer properties in infrastructure projects using DCIP and MRS*

2022, August: Presentation at SGF, Gothenburg. *Geophysical mapping of aquifer properties in infrastructure projects using DCIP and MRS*

2022, October: Presentation at Grundvattendagarna, Gothenburg. *Rumslig kartläggning av grundvattenhydrauliska egenskaper med geofysik*

Cooperation partners and acknowledgements

Within this project, we have cooperated and collaborated with several people and institutes. The Hydrogeophysics Group at Aarhus University/Denmark have done the MRS measurements and analysis and helped with the interpretation and reports (Andrew Kass & Denys Grombacher). The consultant company NIRAS conducted the HPT and slug tests.

The reference group members Christian Butron (Trafikverket), Kristy Heng (Trafikverket), Hans Jeppsson (WSP), Benjamin Andersson (Sweco/Trafikverket) and Nils Pertuu (Geovista) have supported the project with information and contact to the three test sites, their expertise and by providing general comments and suggestions.

During the last two years we also acknowledge the help from Anders Kühl, Aarhus University who has auto processed the DCIP data, Léa Lévy (LTH) who has helped with the visualisation of the final data and the field crew from Lund and Aarhus University (Simon Rejkaer, Matt Griffiths, Mathias Vang). We also thank Johan Månsson, the project leader for test site 1 (Börringe), Hässleholm municipality and the landowner for their support and access to the sites.

References

Dahlin, T. (2001) The development of electrical imaging techniques, Computers and Geosciences, 27(9), 1019-1029.

Danielsen, B.E. and Dahlin, T. (2009) Comparison of geoelectrical imaging and tunnel documentation. Engineering Geology, 107, 118–129.

Fiandaca, G., Maurya, P. K., Balbarini, N., Hördt, A., Christiansen, A. V., Foged, N., et al., 2018. Permeability estimation directly from logging-while-drilling Induced Polarization data. Water Resources Research, 54, 2851–2870. https://doi.org/10.1002/2017WR022411

Fiandaca G., Meldgaard Madsen L., Olmo M., Römhild L., Maurya P.K., 2021. Inversion of hydraulic conductivity from Induced Polarisation, Part A: methodology and verification. Near Surface Geoscience 2021-27th European Meeting of Environmental and Engineering Geophysics, 1-4. Bordeaux, France

Ganerød G.V., Rønning J.S., Dalsegg E., Elvebakk H., Holmøy K., Nilsen B. and Braathen A. (2006) Comparison of geophysical methods for subsurface mapping of faults and fracture zones in a section of the Viggja road tunnel, Norway. Bulletin of Engineering Geology and the Environment, 65, 231 243.

Kirsch R. (2009) Groundwater Geophysics – A Tool for Hydrogeology, ed. 2, Springer, ISBN 978-3-540-88404-0, 548p.

Lachassagne P., Baltassat J.M., Legchenko A. and de Gramont H.M. (2005) The links between MRS parameters and the hydrogeological parameters, Near Surface Geophysics, 3, 259–265.

Liu L., Grombacher D., Auken E. and Larsen J. J. (2019a) Apsu: a wireless multichannel receiver system for surface nuclear magnetic resonance groundwater investigations, Geoscientific Instrumentation, Methods and Data Systems, 8, 1–11.

Liu L., Grombacher D., Auken E. and Larsen J.J. (2019b) Complex envelope retrieval for surface nuclear magnetic resonance data using spectral analysis, Geophysical Journal International, 217(2), 894–905.

Martin T., Flores Orozco A., Dahlin T and Günther T. (2020) Evaluation of spectral induced polarization field measurements in time and frequency domain, Journal of Applied Geophysics, 180, 104141.

Martin, T., Pauw, P.S., Karoulis, M., Mendoza, A., Günther,T., Meldgaard Madsen, L., Kumar Maurya, P., Doetsch, J., Reijkaer, S., Dahlin, T. and G. Fiandaca (2021): “Inversion of hydraulic conductivity from Induced Polarisation, Part B: field examples from five countries”, Near Surface Geoscience 2021-27th European Meeting of Environmental and Engineering Geophysics, Bordeaux, France

Maurya P.K., Balbarini N., Møller I., Rønde V., Christiansen A.V., Bjerg P.L., Auken E. & Fiandaca G. (2018) Subsurface imaging of water electrical conductivity, hydraulic permeability and lithology at contaminated sites by induced polarization. Geophysical Journal International, 213(2), 770–785.

McCall W. & T.M. Christy (2020) The Hydraulic Profiling Tool for Hydrogeologic Investigation of Unconsolidated Formations. Groundwater Monitoring & Remediation, 40 (3), 89-103,

Olsson P.-I., Fiandaca G., Juul Larsen J., Dahlin T. and Auken E. (2016) Doubling the spectrum of time-domain induced polarization by harmonic de-noising, drift correction, spike removal, tapered gating and data uncertainty estimation, Geophysical Journal International, 207(2): 774-784.

Perttu N. (2011) Magnetic Resonance Sounding (MRS) in groundwater exploration, with applications in Laos and Sweden, Dr. thesis, Luleå University of Technology, ISBN 978-91-7439-306-4,39p + appendices.

Rønning J.S., Ganerod G., Dalsegg E. and Reiser F. (2013) Resistivity mapping as a tool for identification and characterisation of weakness zones in crystalline bedrock: definition and testing of an interpretational model. Bulletin of Engineering Geology and the Environment, 73(4), 1225–1244.

TRV (2020a) E65 Svedala-Börringe -Tekniskt PM, Hydrogeologi, Svedala kommun, Skåne 2020-11-27 Projektnummer: 148277. Report Trafikverket

TRV (2020b) E20 Förbi Mariestad, delen Muggebo-Tjos, Projekterings PM, Hydrogeologi Projektnummer: 150307, Report Trafikverket

Weller, A., Slater, L., Binley, A., Nordsiek, S., & Xu, S. (2015). Permeability prediction based on induced polarization: Insights from measurements on sandstone and unconsolidated samples spanning a wide permeability range. Geophysics, 80(2), D161–D173.

Weller A. and Lee Slater L. (2019) Permeability estimation from induced polarization: an evaluation of geophysical length scales using an effective hydraulic radius concept, Near Surface Geophysics, 17, 581–594.